Exploring the Hadronic Axion Window via Delayed Neutralino Decay to Axinos at the LHC

C.S. Redino[1,*] and D. Wackeroth[1,†]

[1]*Department of Physics, SUNY at Buffalo, Buffalo, NY 14260-1500, USA*

(Dated: December 22, 2015)

arXiv:1512.06822v1 [hep-ph] 21 Dec 2015

Abstract

The addition of the QCD axion to the Minimal Supersymmetric Standard Model (MSSM) not only solves the strong CP problem but also modifies the dark sector with new dark matter candidates. While SUSY axion phenomenology is usually restricted to searches for the axion itself or searches for the ordinary SUSY particles, this work focuses on scenarios where the axion's superpartner, the axino, may be detectable at the Large Hadron Collider (LHC) in the decays of neutralinos displaced from the primary vertex. In particular, we focus on the KSVZ axino within the hadronic axion window. The decay length of neutralinos in this scenario easily fits the ATLAS detector for SUSY spectra expected to be testable at the 14 TeV LHC. We compare this signature of displaced decays to axinos to other well motivated scenarios containing a long lived neutralino which decays inside the detector. These alternative scenarios can in some cases very closely mimic the expected axino signature, and the degree to which they are distinguishable is discussed. We also briefly comment on the cosmological viability of such a scenario.

*Electronic address: csredino@buffalo.edu

†Electronic address: dow@ubpheno.physics.buffalo.edu

I. INTRODUCTION

Supersymmetry (SUSY) [1, 2] is a well-motivated framework for physics beyond the Standard Model (SM) near the weak scale (see, e.g., [3–7] for a review), with attractive features such as a solution to the weak-scale gauge hierarchy problem in the SM, the possibility of gauge coupling unification, and an apparent dark matter (DM) solution. The lightest neutralino in the Minimal Supersymmetric SM (MSSM) acting as a weakly interacting massive particle (WIMP) provides approximately the correct cold DM (CDM) relic abundance (for a review see, e.g., [8]). This so-called "WIMP miracle" in SUSY is often overstated, however, in that there can still exist a tuning of SUSY parameters in order to get the correct abundance, SUSY models with the correct abundance only constitute a very small fraction of SUSY model space, and models that over or under predict the DM relic abundance are common [9–13]. Simply by virtue of reducing the available parameter space, the requisite of a DM solution can exclude more natural scenarios in SUSY [11].

The additional constraints and tuning introduced by accommodating DM in a SUSY model can be avoided by extending the dark sector beyond just neutralinos, but it is desirable to do this in a way that is minimal and well motivated in of itself. The neutral, pseudoscalar, R-parity even axion is an attractive candidate for an extended dark sector because it has motivation beyond its properties as a DM particle. The Peccei-Quinn (PQ) axion's origins are independent of any considerations of DM, originally introduced to resolve an apparent fine-tuning problem in the SM QCD sector, known as the strong CP problem [14, 15]. The strength of the axion's interactions is suppressed by the PQ scale f_a. When f_a is sufficiently large the axion becomes a viable DM candidate [16–18].

The role of the axion as a DM candidate in a SUSY model can be more complicated than simply complimenting the neutralino relic abundance. Embedded in a SUSY model, the axion is a member of a supermultiplet, joined by a neutral, R-parity odd Majorana chiral fermion, the axino [19, 20], and the R-parity even scalar saxion [21]. Also the axino is a viable DM candidate [22] and can provide the correct CDM relic abundance [23–26]. With the neutralino, axion and axino being all valid DM candidates (see, e.g., [12] for a recent review), which particle (or set of particles) actually plays the role of DM in a given model depends on their mass hierarchy and the cosmology, so there are a variety of possible scenarios. The scenarios in such a PQ-augmented MSSM (PQMSSM) have been studied

extensively in [27–31], where it has been pointed out that there exist significantly more scenarios than in the MSSM that predict the correct CDM abundance. Apart from solving the strong CP problem, the PQMSSM can have other benefits such as Yukawa unification [32] or being embedded in a full GUT theory [33]. Moreover, scenarios in the PQMSSM often have an easier time accommodating naturalness in SUSY, if for nothing else then because an extended model has more parameters and is more flexible.

These attractive features of a PQMSSM warrant an extensive study of all aspects of its phenomenology. While SUSY axion phenomenology is usually restricted to searches for the axion itself or searches for the ordinary SUSY particles, this work focuses on scenarios where the axion's superpartner, the axino, may be detectable at the Large Hadron Collider (LHC). In particular, we focus on the Kim-Shifman-Vainshtein-Zhakharov (KSVZ) [34, 35] axion model, and consider the axino to be the lightest SUSY particle (LSP) produced at the LHC in neutralino decays displaced from the primary vertex. The latter can happen when the PQ scale f_a is in the range known as the hadronic axion window [36]. The decay length of neutralinos in this scenario easily fits the ATLAS detector for SUSY spectra expected to be testable at the 14 TeV LHC. We explore the possibility of distinguishing this axino collider signature from other well motivated scenarios containing a long lived neutralino but no axino LSP. Examples of alternate collider signatures of axino LSPs, for instance in displaced charged slepton decays and in prompt or displaced Higgsino decays can be found in respectively [37] and [38] (see Section II for a more detailed discussion). To make the collider phenomenology of the model under consideration in this work possible at all requires certain assumptions about the axion model and the SUSY spectra, which makes this scenario distinct from those already studied, but nonetheless it is a predictive scenario with the possibility of low tuning, and compatibility with an attractive cosmology.

The rest of the paper is organized as follows: In Section II, we discuss what assumptions are necessary for an axion model so that collider phenomenology is possible. In Section III, we discuss the proposed signal and an example SUSY benchmark model with parameters that put this signal within reach at the 14 TeV LHC. In Section IV, we compare this signal in detail to other similar possibilities from gravitinos and R-parity violation (RPV). A discussion of how the scenarios under study can accommodate the correct DM abundance can be found in Section V. Lastly we conclude by considering the limitations of this work and how it can be expanded in the future. A greatly expanded discussion of the proposed

scenario and the results in this study can be found in [39].

II. MOTIVATION AND ASSUMPTIONS

The usual wisdom that prevents axinos from being considered for collider phenomenology is their extremely weak coupling. All the couplings of the axion are suppressed by the PQ scale f_a, which in theory can take any value. Axions as CDM candidates are usually only considered with 10^9 GeV $< f_a < 10^{14}$ GeV [40]. For an axion to be the Pseudo-Nambu-Goldstone boson of a spontaneously broken global $U(1)$ chiral symmetry to solve the strong CP problem, the axion field ($a(x)$) described as follows [14] (for a review see, e.g., [15]):

$$\mathcal{L}_{axion} = -\frac{1}{2}\partial_\mu a(x)\partial^\mu a(x) + \mathcal{L}_{int}(\partial^\mu a/f_a;\Psi)) + \xi\frac{a(x)}{f_a}\frac{\alpha_s}{8\pi}F_b^{\mu\nu}\tilde{F}_{b\mu\nu}\,, \tag{1}$$

has an effective potential that has a minimum at $< a >= -\frac{f_a}{\xi}\bar{\theta}$. $F_b^{\mu\nu}$ is the gluon field strength tensor, and $\tilde{F}_b^{\mu\nu}$ its dual. Thus, with $a_{phys} = a - < a >$ the CP-violating $\bar{\theta}$-vacuum term in $\mathcal{L}_{QCD}$ is canceled. As can be seen in Eq. 1, the coupling strength of the axion to the SM particles is governed by f_a with f_a being a free model parameter, only determined by experimental and observational constraints. A summary of all the current constraints on f_a is shown in Fig. 1 [41].

The model-dependent nature of these limits can be exploited to conceive models appropriate for collider phenomenology, but first it is worth considering why the typical limits are so restrictive. If the usual lower bound of $f_a > 10^9$ GeV is taken at face value then collider studies for axions (or equally suppressed axinos) are very limited. Direct production rates of axions/axinos are simply too small with such a suppressed coupling, but an incredibly weak coupling may still be probed in certain cases, usually by taking advantage of R-parity. If an extremely weakly coupled particle (such as an axino or gravitino) is the lightest particle with an odd R-parity then their appearance at the end of a SUSY decay chain is inevitable, regardless of the coupling size. One way to take advantage of this is if the next-to-lightest SUSY particle (NLSP) is charged, then its delayed decay to the suppressed LSP will leave a track (see, e.g., Ref. [37]). Even with neutral NLSPs, R-parity can still be exploited in much the same way to look for extremely weakly coupled particles, but with a less spectacular signal. R-parity still requires the LSP to be at the end of any SUSY decay chain, and while there is no longer a charged track, the visible decay products in the last leg will be displaced.

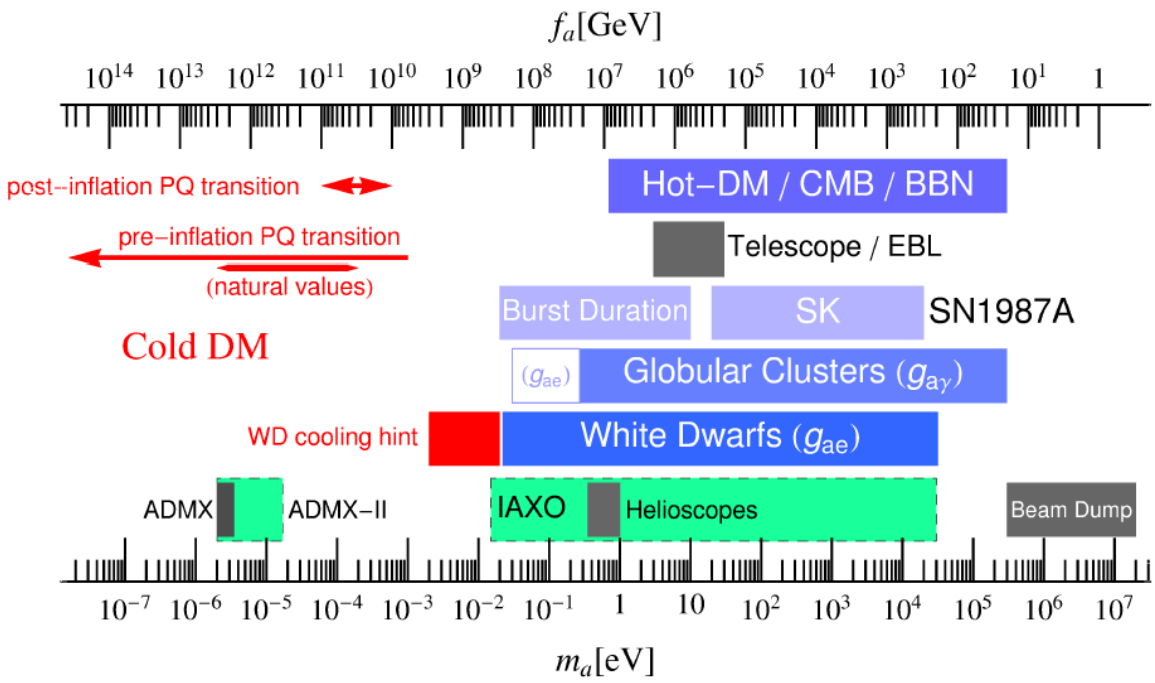

FIG. 1: Exclusion ranges for the Peccei-Quinn scale f_a (and the related axion mass m_a) from various constraints as described in [41]. A critical discussion of these constraints in the scenario considered in this work can be found in the text.

Even though R-parity forces a branching fraction of one for the LSP, the very weak coupling of the LSP still has an effect: in determining the width of the NLSP which translates to how displaced the last leg of the SUSY cascade will be. If the suppression factor is great enough, then the displaced decay occurs completely outside the detector, and so the scenario is indistinguishable from one without the extra particle in the final leg at all. If these types of searches are taken seriously for gravitinos (and they are [42, 43]), one would hope that this could be exploited for axinos, but there are a couple of technical differences that make this difficult. Naively one would assume these searches are even harder for gravitinos since their interactions are suppressed by the Planck scale, which dwarfs even the higher values of f_a that are considered in the literature. While the gravitino's interactions are suppressed by the Planck scale, they are also inversely proportional to the gravitino mass and so the suppression is not as great as one may naively expect [44]. In effect, the coupling strength can be tuned to any value provided there is freedom in choice of the gravitino mass (which can take a wide range of values depending on the model). For extremely small gravitino masses,

searches for displaced or even prompt decays of NLSPs become possible. In displaced decays to axinos, the effective coupling is relatively insensitive to the axino mass and only depends strongly on f_a and any axino with $f_a > 10^9$ GeV is expected to be completely invisible at colliders, as any decaying NLSP will always leave the detector [45]. Very recently an exception to this common wisdom was explored in [38], where the authors showed that a Higgsino NLSP can decay to an axino LSP inside the detector easily even with $f_a > 10^9$ GeV, when there is a direct coupling between Higgsinos and axinos (and an appropriate mass spectrum) as in the case of Dine-Fischler-Srednicki-Zhitnitsky (DFSZ) axions [46, 47].

For DFSZ axions, displaced decays of a neutral NLSP are possible because of the coupling between axinos and Higgs bosons/Higgsinos, but for the other main class of axion model, the KSVZ axion, it seems that collider studies are only possible, if the constraints on f_a can be relaxed.

Limit plots, such as Figure 1, where all the constraints are given in terms of f_a, often do not easily reveal the underlying model-dependent assumptions in extracting these constraints. After closer inspection, it turns out that in the KSVZ model there is the intriguing possibility of evading most of the constraints in a way not possible in the DFSZ model. In the KSVZ model the axion coupling to leptons is vanishing at tree level, and the effective coupling to leptons at one loop has been shown to be non-constraining [48, 49]. As a result, a whole category of constraints, i.e. the limits from white dwarf cooling, are irrelevant for the KSVZ axion when $g_{ae} = 0$ in Fig. 1. In the DFSZ model, the coupling to leptons is always non-vanishing. Aside from the white dwarf limits, the coupling most often tested is the axion coupling to photons, given by

$$\mathcal{L}_{a\gamma\gamma} = \frac{\alpha}{4\pi} K_{a\gamma\gamma} \frac{a_{phys}}{f_a} F^{\mu\nu} \tilde{F}_{\mu\nu} \, . \tag{2}$$

where $F^{\mu\nu}$ is the photon field strength tensor and $K_{a\gamma\gamma}$ parameterizes the model-dependent axion-photon coupling. This too can be made to vanish in the KSVZ model (but not the DFSZ). In the KSVZ model the coupling to photons is determined by [48, 49]

$$K_{a\gamma\gamma} = K^0_{a\gamma\gamma} - \frac{2(4+z)}{3(1+z)} \, , \tag{3}$$

and the difference can be thought of as a balancing between short and long-range effects. The short-range effect $K^0_{a\gamma\gamma}$ comes from the chiral anomaly depending on the electromagnetic charge(s) of the new heavy quark(s) that are required for UV completion in KSVZ models.

The second term in Eq. 3 comes from the axion's mixing with light mesons and depends on the value of z, the ratio of light quark masses ($z = m_u/m_d$), which comes with some uncertainty ($z = 0.38-0.58$ [41]). For an appropriate choice of charge(s) for the new quark(s) these two terms can cancel and $K_{a\gamma\gamma}$ can be made to vanish [48, 49]. It should be noted that to avoid the existing constraints $K_{a\gamma\gamma}$ does not have to vanish exactly, but only be so small that it is consistent with the limits on the photon coupling. Once $g_{a\gamma} = 0$ is assumed the constraints originating from globular clusters and from telescope searches for $a \to \gamma\gamma$ in Fig. 1 are no longer valid. Also current and anticipated constraints from the search for solar axions at CAST [50], and IAXO [51] rely on a non-zero axion-photon coupling.

Thus, for a KSVZ axion with no photon or lepton coupling ($g_{ae} = 0$ and $g_{a\gamma} = 0$ in Fig. 1), the only constraints in Figure 1 that are truly inescapable are those coming from SuperNova (SN) 1987a [52, 53]. In practice, the new light species do not even have to be detected from these events, but their properties can be constrained from the burst duration of the supernova, and the number of particles detected from the light species of the Standard Model (neutrinos). In the case of QCD axions this is especially interesting because it directly tests the otherwise elusive gluon-axion coupling, the only coupling necessary to solve the strong CP problem, and the only coupling free from model dependent factors. As seen in Figure 1, there are actually two separate regions of bounds from SN1987a, corresponding to two regimes of coupling strength. The upper bound range comes from when the axion is so weakly coupled that it is free streaming after it is produced in the supernova and the lower bound range is from axions that still have interactions with nuclear material on there way out of the supernova. If the photon coupling is taken to vanish (or be adequately suppressed), then there is a gap in the constraints between the two regimes of free streaming and interacting axions in Supernovae. This window allows a range of lower suppression scale $3 \times 10^5\text{GeV} < f_a < 3 \times 10^6\text{GeV}$, known as the hadronic axion window, which has been examined in the literature in the past, particularly in the context of axions as hot dark matter and its cosmological implications [36, 54]. Though hot dark matter is now greatly disfavored, axions in this window, though still relatively suppressed by f_a, should have coupling strengths such that their partners, the axinos, can be studied at colliders, via the general strategy for gravitinos and displaced decays described above. The hot dark matter bound in Figure 1 is the usual reason why the hadronic axion window is considered "ruled out", which comes about from there being too much of a hot thermal relic of axions

in conflict with measurements of large scale structure and the CMB, but at least one way to avoid this is by considering cosmologies with a very low reheating temperature. Although the hot dark matter bound is model independent with regards to the axions themselves, it is model dependent as far as the cosmology is concerned. A dangerous hot thermal relic in one cosmology can be made safe in another cosmology with a lower reheating temperature. Standard Model neutrinos were shown to be a viable warm dark matter candidates with this method in [55] and the same principle has been applied to axions to alleviate constraints [56]. By lowering the reheating temperature sufficiently, thermal relics freeze out while the universe is still undergoing inflation, and the relic abundance will be diluted. Diluting the thermal axion abundance sufficiently in a scenario where f_a is in the hadronic axion window would evade constraints, but could also require an additional species of dark matter, such as an axino.

With these assumptions laid out, the scenario to be studied at the LHC should be clear: KSVZ axinos with a neutral NLSP, with only a QCD coupling, and the suppression scale, f_a, to be considered lying in the range given by the hadronic axion window:

$$3 \times 10^5\,\mathrm{GeV} < f_a < 3 \times 10^6\,\mathrm{GeV}$$

This scenario is motivated by being perhaps the only KSVZ model that is testable at a collider without a charged NLSP. This scenario also has the possibility of having low tuning and an interesting cosmology with its own testable consequences. In Section V, we will provide an estimate of the DM abundance due to thermal/non-thermal axions and axinos in this model.

III. SIGNAL AND BENCHMARK

In the following we will concentrate on PQMSSM scenarios with a neutralino NLSP. With only the effective coupling to gluons being allowed in the hadronic axion window, this makes for a very predictive scenario.

The supersymmetric version of the axion-gluon coupling is the axino-gluino-gluon coupling [28],

$$\mathcal{L}_{\tilde{a}\tilde{g}g} = i\frac{\alpha_s}{16\pi f_a}\bar{\tilde{a}}\gamma_5[\gamma^\mu,\gamma^\nu]\tilde{g}_b F_{b\mu\nu} \tag{4}$$

and is the only coupling available to produce axinos in this scenario. $\tilde{a}$ and $\tilde{g}_b$ denote the axino and gluino field respectively. Even within the window of lower f_a considered here, the suppression is still too large to expect production of axinos at the LHC unless they follow the NLSP in a decay chain so that there are no other less suppressed options for decay. Once a neutralino is produced there is only one dominant topology for its decay to an axino at tree level (Fig. 2), via an off shell squark and an off shell gluino, resulting in missing transverse energy (MET) and three displaced jets, (plus whatever SM particles were produced in association with the neutralino). This topology allows decays to heavy quarks, but the decay width should be relatively small compared to that of decays to light quarks, provided the neutralino is not too massive. At tree level this is the only topology that leads to four decay products and there are no topologies with a smaller multiplicity. Any other decay path from neutralino to axino involves more final state particles and possibly more massive off shell sparticles in the decay chain, and so the process is even more greatly suppressed to the point where it is negligible compared to the three displaced jets and MET channel.

It is very important however to consider one-loop effects here. The vertex correction to squarks decaying to axinos, shown in Figure 3, provides an effective squark-quark-axino coupling that can provide the dominant decay channel for neutralinos for large swathes of SUSY parameter space. This effective coupling was first explored in [57], and with the heavy states integrated out, this interaction takes the form

$$\mathcal{L}_{\tilde{a}q\tilde{q}} = -g_{eff}\tilde{q}_j^{L/R}\bar{q}_j P_{R/L}\tilde{a} \ , \tag{5}$$

where $m_{\tilde{g}}$ is the gluino mass, $\bar{q}_j$ and $\tilde{q}_j^{L/R}$ is the quark and (left or right-handed) squark field respectively, and $P_{R/L} = (1 \pm \gamma_5)/2$, and the effective coupling

$$g_{eff} \simeq \frac{\alpha_s^2}{\sqrt{2}\pi^2}\frac{m_{\tilde{g}}}{f_a}\log\left(\frac{f_a}{m_{\tilde{g}}}\right) \ . \tag{6}$$

With this effective coupling considered, there is the possibility of neutralino decay to an axino and two jets (Figure 4), and this is the decay channel we focus on here. The relative strength of $\mathcal{L}_{\tilde{a}\tilde{g}g}$ and $\mathcal{L}_{\tilde{a}q\tilde{q}}$ was explored in [57] with regards to squark decays, where it was shown that the $\mathcal{L}_{\tilde{a}q\tilde{q}}$ decay dominates unless $m_{\tilde{q}} \gg m_{\tilde{g}}$. This also holds true here, where neutralino decays are mediated by an off-shell squark. The decay width for $\tilde{\chi}_j^{(0)} \to q\bar{q}\tilde{a}$ is discussed in more detail in Section IV A.

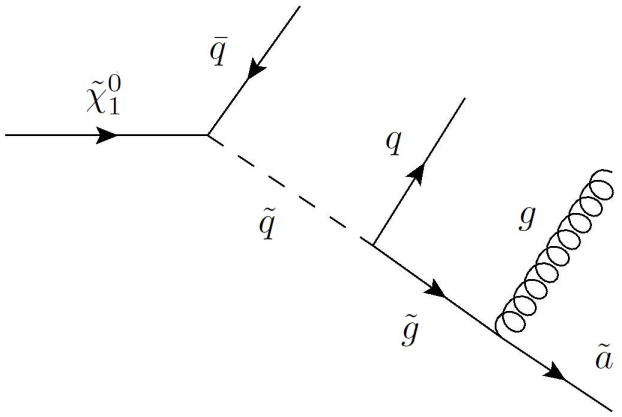

FIG. 2: Neutralino decay to three jets and an axino via $\mathcal{L}_{\tilde{a}\tilde{g}g}$ of Eq. 4.

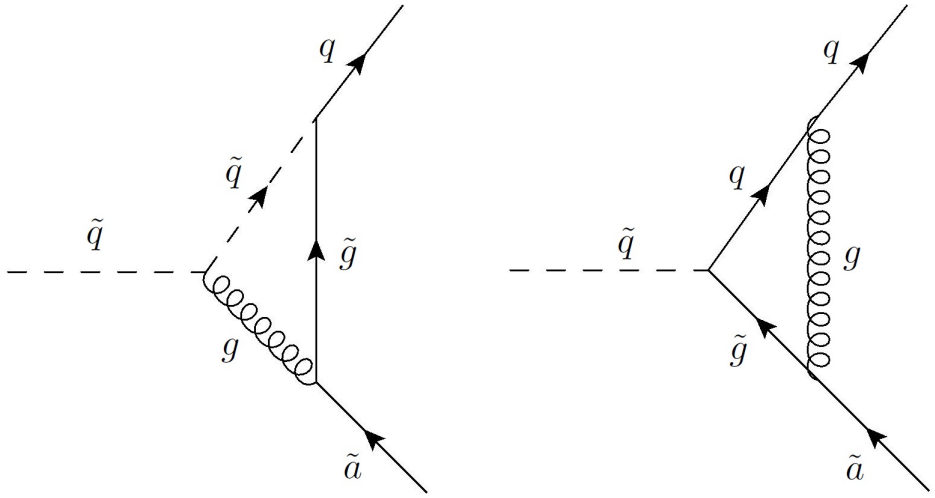

FIG. 3: The vertex corrections that lead to the effective squark-quark-axino interaction, $\mathcal{L}_{\tilde{a}q\tilde{q}}$ of Eq. 5.

For two produced neutralinos decaying to axinos, the signal is always multi-jets and MET, and depending on the SUSY spectra the dominate decay will either be two or three jets per decay leg (before showering/clustering). Multi-jets and MET is by far the most commonly studied signal for prospective new physics at the LHC, but if the jets are displaced enough, then the signal for KSVZ axinos with a neutralino NLSP can become rather unique. If the jets are displaced enough when neutralinos decay then the SM background will become negligible, and the only competing or alternative source for such a signal would come from

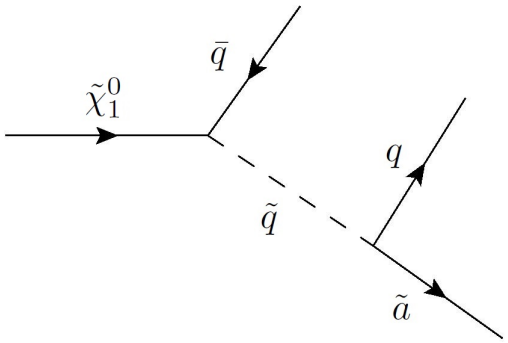

FIG. 4: Neutralino decay to two jets and an axino via $\mathcal{L}_{\tilde{a}q\tilde{q}}$. of Eq. 5.

other new physics. Two such alternative sources are displaced decays of neutralinos to gravitinos and displaced decays of neutralinos to neutrinos via RPV. These two alternative sources may not only arise in alternative models, but could all exist consistently in one model, i.e, a model with axinos, light gravitinos and RPV couplings all at once is allowed. There would have to be a coincidence of scales for there to be a sizable branching fraction for the neutralino to each of these, instead of one mode dominating. Distinguishing between these sources of highly displaced jets is left to the next section, but for now it should be noted that these types of searches have already been considered in the literature for gravitinos [58] and RPV [59], and these studies can be used as a guide for what can be done with axinos. Besides removing the SM background, highly displaced jets also allow the SUSY production channel and the signal to be discussed independently. Regardless of how neutralinos are produced, either in a simple two to two process, or at the ends of various long cascade chains, the multi-jet signal is relatively unchanged, so long as the displaced jets are what is triggered on. This means that optimistically, the rate of the displaced jets signal can be taken as the inclusive SUSY production rate for a given benchmark. There are however, a few ways the production mechanism will effect the signal, even for highly displaced jets. Exclusive neutralino pair production will produce the most highly boosted jets, with longer and longer decay chains reducing the amount of boost, though this is likely a small effect. In addition to this distribution of boosts, the rest of the SM particles produced in decay chains must be considered when determining the MET of the whole event, and the MET resolution may vary between decay chains. Another effect to consider is that the triggers for highly displaced objects usually have isolation requirements, so that the production channel for neutralinos must not produce calorimeter activity in a region that points to the displaced

decay.

While there are these advantages to considering highly displaced jets, the drawback is that jet measurements may be difficult in the outer parts of the detector. The degree to which detailed reconstruction of jets in the outer detector is possible is beyond the scope of this work, but at least it should be noted that in similar searches, such as displaced decays to gravitinos [58], the strategy is to make use of triggers developed for hidden valley searches at ATLAS [60]. The hope is that these same triggers could be used for displaced decays to axinos. ATLAS has an advantage here simply because of the detector geometry: a larger detector has a chance to detect particles with longer decay lengths. A hidden valley can produce displaced jets very similar to gravitinos or axinos, but the hidden valley is not a particular model, or even frame work of models, but rather a feature that can arise in various settings, so no attempt is made in this work to make a direct comparison between a hidden valley signal and other neutralino decays.

With the expected signal identified as displaced jets and MET, the SUSY spectra must be specified to obtain more quantitative results. An appropriate benchmark SUSY model should meet a few criteria. Two such benchmark models are chosen here, so that in Section IV the effect of varying kinematics on the distributions can be explored. Model 188924 and 2178683, both proposed as PMSSM benchmarks for Snowmass 2013 [61] are appropriate and appealing for several reasons. The spectra of these models are given in Figures 5 and 6. The important difference between these two models is that model 188924 has a lighter LOSP neutralino, a bino near 200 GeV, and here it will be referred to as the "lighter" benchmark, while model 2178683 also has an LOSP bino, but a bit heavier, closer to 500 GeV in mass and will be referred to as the "heavier" benchmark. Both models have colored sparticle masses all between 1 TeV and 4 TeV. These masses are the relevant model parameters to the topology in Figure 4, along with the neutralino mixing and the PQ scale, f_a.

The 19 parameter PMSSM makes no assumptions about the high scale theory of supersymmetry and only specifies parameters at a low scale. While it is more flexible then a SUSY model that specifies how SUSY is broken, such as Minimal Super Gravity (MSUGRA) or GMSB, it can also contain these models as a subset. Besides being agnostic to high scale physics, this set of benchmarks was chosen by the authors as being testable at a 14 TeV LHC and has been tested thoroughly so that it evades the gauntlet of existing searches up to this point. Many SUSY models can evade existing constraints, but this model does not

implement any special considerations to do so, it is simply the result of a scan of the large PMSSM parameter space, and so can be thought of as a "generic" SUSY model that may be realized in the next run of the LHC. All the models in this collection are stated to have possible dark matter candidates, in that they do not over saturate the relic abundance, but this point is moot in this context since the neutralino LOSPs will all decay to axinos in the scenario here. In addition to these features which are common to all of the PMSSM benchmarks described in [61], the benchmarks for this specific scenario of neutralino decays to axinos requires a few more features. The total neutralino width should be in a range such that the decay is clearly displaced from the primary vertex, but still within the ATLAS detector. The range considered appropriate for this is between 0.1 m and 10 m. The analysis is also easier if only one of the two possible decays (two jet or three jet per leg) is clearly dominant, so that there is no issue of double counting and matching with the number of jets. For both the lighter and heavier benchmarks chosen here with a gluino heavier than most of the squarks, the 3 jet channel is suppressed by several orders of magnitude compared to the 2 jet channel, so that the only coupling that needs to be considered is $\mathcal{L}_{\tilde{a}q\tilde{q}}$ of Eq. 5 and the only relevant topology is that shown in Figure 4. Also, with neutralinos in this mass range, the branching fraction to heavy quarks is greatly suppressed so that the neutralino branching fraction to two light jets and an axino is very nearly one. There should also be an adequate rate for a signal, which optimistically can be taken as the inclusive SUSY rate. At the 14 TeV LHC the total inclusive SUSY cross section for the lighter model benchmark is $\sigma_{SUSY} = 5.4$ fb, and for the heavier one is $\sigma_{SUSY} = 23$ fb, as obtained at leading-order with MadGraph/MadEvent [62]. Several of the benchmarks in this collection actually satisfied all of these criteria, and the lighter benchmark model 188924 was only chosen because it has the added appeal of relatively light sparticles, especially with relatively light Higgsinos near 270 GeV, indicating that this benchmark may have lower tuning. The heavier benchmark was simply chosen because a heavier neutralino will have an impact on the kinematic distributions used to distinguish between different neutralino decays (axino/gravitino RPV) as will be shown in Section IV.

Several SUSY masses and parameters are not specified in these benchmarks. The gravitino, for the purposes of this study, will be assumed to be heavy enough that it does not effect the collider phenomenology. Note that this does not have to be very heavy, as only very light gravitinos are expected to not escape the detector. Gravitinos heavy enough to

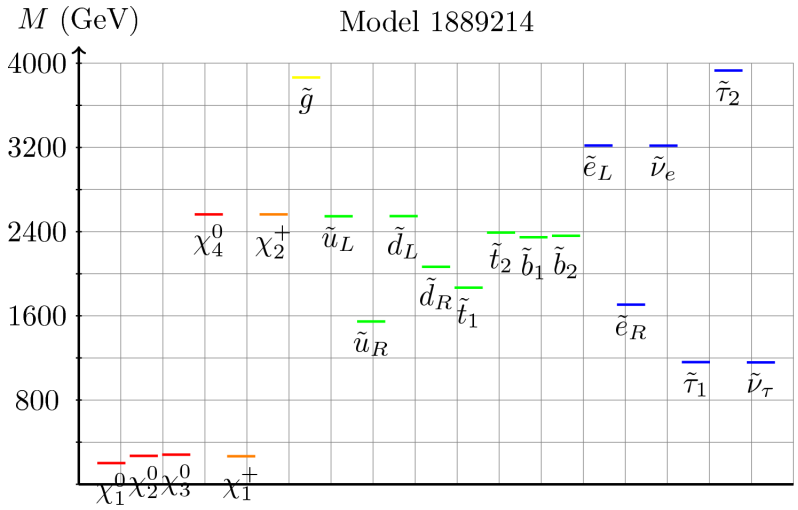

FIG. 5: The "lighter" benchmark with an LOSP bino at ≈ 200 GeV, taken from [61].

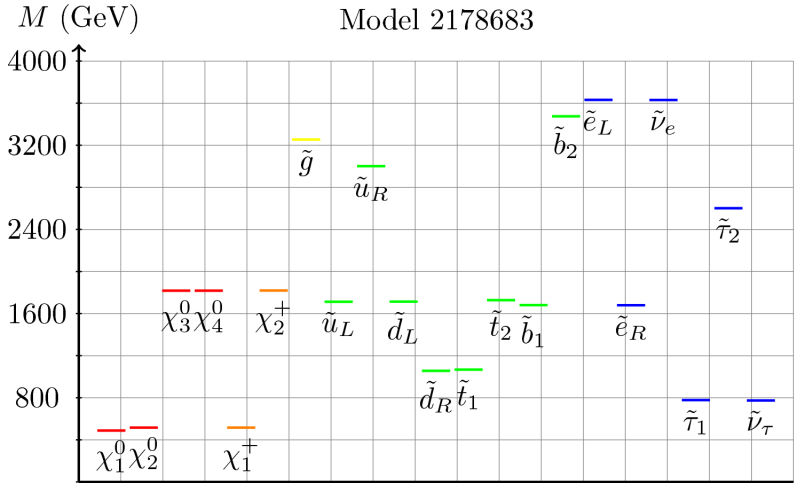

FIG. 6: The "heavier" benchmark with an LOSP bino at ≈ 500 GeV, taken from [61].

decouple from collider physics can still have a large effect on the cosmology. The only remaining masses are those from the axion supermultiplet. The KSVZ axions mass is directly determined by the scale f_a so in the hadronic axion window these axions are still very light, with a mass of approximately 10 eV. The axion is still too weakly coupled to have an effect on collider studies, and since it is R-parity even, there are no tricks to apply as in the case of the axino. The scalar saxion's mass is model dependent, but it is not expected to effect collider phenomenology, because like the axion, it has even R-parity. Like the gravitino, the saxion can still greatly affect the cosmology without changing collider studies. Finally, the object of interest, the axino does not yet have a specified mass. Theoretically the axino mass

is highly model dependent and a large range of values are explored in the literature, so it can be taken as a free parameter here. As an LSP, lighter axinos are preferred so they are not over-produced in the early universe [63], but this will be somewhat alleviated if we assume a low reheat cosmology as mentioned in the previous section. The signal of displaced jets and MET is expected to be insensitive to the axino mass for relatively light axinos. As the axino becomes heavy enough the width of the NLSP will be affected, which will be explored in more detail in Section IV A.

The signal for KSVZ axinos with a neutral NLSP at the LHC is very predictive in that there are only two couplings to consider, each providing one dominate topology. For this first study, the benchmarks chosen have spectra that seems appropriate in that they are relatively generic (the result of scans and not specifically "engineered") and they are expected to give decay lengths in an appropriate range. Beyond these particular benchmarks, the mixing of the NLSP neutralino, the amount of compression of the spectra, and the mass of the axino may affect the signal to some degree and it is worth testing. Though there are no SM backgrounds to compete with very displaced jets, there are other possible decays for the neutralino, including decays to gravitinos and decays via RPV. Now that these qualitative aspects of the signal have been summarized, in the next section results are presented for simulated events, for decays to axinos and the alternatives. The impact of the possible effects described above are explored and the degree to which these neutralino decays can be distinguished is tested.

IV. RESULTS AND DISCUSSION

To investigate how predictive the axino multi-jet and MET signal is, we simulated events for the LHC at 14 TeV. The primary tool used to generate Monte Carlo events was MadGraph/MadEvent [62]. The parton distribution function (PDF) set used with MadEvent was CTEQ6L1 [64]. The renormalization and factorization scales were allowed to run and were determined by MadEvent's default settings with the scale for decay events set to the mass of the decaying parent particle. We added the axino field and its couplings to the MSSM using FeynRules [65–67]. The FeynRules implementation of the axino was validated for $\mathcal{L}_{\tilde{a}\tilde{g}g}$ of Eq. 4 by comparing the tree level decay of a heavy axino to the analytical result, and for $\mathcal{L}_{\tilde{a}q\tilde{q}}$ of Eq. 5 by comparing the squark decay width to the results in [57]. We also

calculated the neutralino decay width for $\tilde{\chi}^{(}0)_j \to q_i \bar{q}_i \tilde{a}$ analytically and confirmed the result of [68] with the appropriate adjustments (see Eq. 8), and used this analytic form of the decay width to verify the results obtained with MadGraph/MadEvent.

Existing model files in the FeynRules data base were used when generating comparison events for the cases with gravitinos [69] and RPV couplings [70]. Mass spectra were generated using SoftSusy [71] and checked with SuSpect [72]. Jet clustering was done with FastJet [73] using kT jets with $D = 0.4$, and parton showers were generated by Pythia [74]. The analysis is done in Mathematica with the Chameleon package [75] as a base, but with plenty of modifications and extensions. Examples of Mathematica notebooks for event analysis with the Chameleon package including these modifications can be found at [76]. Events are generated at tree level, but the vertex correction of Fig. 3 is captured in the effective coupling in $\mathcal{L}_{\tilde{a}q\tilde{q}}$ of Eq. 5.

The only tool required for this study which is less common was evchain [77] which acts as a "MadGraph manager" to combine separate subprocess runs, and is especially useful for decay chains which are difficult for MadGraph to manage alone. In this scenario with axinos, MadGraph has difficulty because of the extremely narrow decay width of the neutralino. As described in the previous section, there is effectively only one topology by which the neutralino can decay, i.e. to two jets and the axino. While the branching fraction to two jets and the axino is very close to one, the width is still extremely small because of both the suppression from the presence of f_a in the denominator and because of the heavy off-shell squark required for the decay. MadGraph can generate the decays of the neutralino just fine, but to include these decays in a larger event is problematic.

Looking at just the neutralino decay alone, the decay width is calculated from which the expected decay length $c\tau$ in the detector is determined, so the assumption that there are plenty of highly displaced jets can be tested. For the lighter benchmark of Figure 5 with a light axino, the width of the lightest neutralino varies between $\Gamma_{\tilde{\chi}_1^0} = 7.3 \times 10^{-16}$ GeV and $\Gamma_{\tilde{\chi}_1^0} = 1.7 \times 10^{-17}$ GeV over the window $3 \times 10^5 \text{GeV} < f_a < 3 \times 10^6 \text{GeV}$. This corresponds to a mean decay length range between roughly $c\tau = 0.26$ m and $c\tau = 11.6$ m. For the heavier model Figure 6 over the same range in f_a the neutralino width spans the range $\Gamma_{\tilde{\chi}_1^0} = 1.7 \times 10^{-13}$ GeV and $\Gamma_{\tilde{\chi}_1^0} = 1.2 \times 10^{-15}$ GeV or a length range of $c\tau = 0.0012$ m and $c\tau = 0.16$ m. This range is a very appropriate size for the ATLAS detector, allowing for a sizable number of events that are displaced enough to realize the advantages described

in the previous section: negligible SM backgrounds, and the ability to separate particles from production and particles from neutralino decay. This width is also insensitive, i.e. within statistical errors, to the axino mass in the range $0 \leq m_{\tilde{a}} < 10$ GeV. The hope is that the axino signal would be trigger-able at this depth in the ATLAS detector using the hidden valley triggers discussed in [60]. No serious attempt is made here at determining the efficiency of such triggers for this model, as adjusting for instance, detector simulation tools for displaced jets is non-trivial work, and not readily available in off-the-shelf tools, but Meade *et al.* do make an estimate of the efficiency of some of these triggers for highly displaced jets in [58].

For the remainder of events analyzed the axino is assumed to be very light (effectively massless) and $f_a = 10^6$ GeV, corresponding to a neutralino decay width of $\Gamma_{\tilde{\chi}_1^0} = 1.1 \times 10^{-16}$ GeV for the lighter benchmark and $\Gamma_{\tilde{\chi}_1^0} = 7.5 \times 10^{-15}$ GeV for the heavier benchmark.

If the trigger can actually be agnostic to the production mechanism, then all SUSY channels can contribute to the signal cross section, and for the benchmark this gives an inclusive SUSY rate of $\sigma_{SUSY} \sim 5$ fb for the lighter benchmark and $\sigma_{SUSY} \sim 23$ fb for the heavier one. In the much more pessimistic case where we only attempt to look for events with neutralino decays only, i.e. neutralino pair production, then the rate is only $\sigma_{\tilde{\chi}_1^0\tilde{\chi}_1^0} \sim 30$ ab for the light benchmark and $\sigma_{\tilde{\chi}_1^0\tilde{\chi}_1^0} \sim 14$ ab for the heavy one, possibly providing just a few events with $\mathcal{L} = 300\,\text{fb}^{-1}$, if they survive the efficiency of the triggers (note that the HL-LHC is designed to reach $\mathcal{L} = 3\,\text{ab}^{-1}$).

Looking at simulated events for the decay alone is still useful for studying the shapes of the kinematic distributions. Even though the neutralino decays actually will occur after some production process with boosted momentum and convolution with PDFs, the distributions from decay-only events are still physical in that they show the relevant observables in the neutralino rest frame. These rest-frame distributions can provide interesting hints as to how the lab-frame distributions may be distinguished between different neutralino decays (axino/gravitino/RPV). More optimistically, these rest-frame distributions may be directly accessible, if the neutralino momentum in the lab frame can be reconstructed, then the appropriate boost on the lab-frame observables can be made. Such a boosting is not a simple task for partially invisible decays, and no explicit algorithm is provided here, but similar reconstruction for partially invisible decays has been done for instance in the context of top decays [78]. Cleaner distributions (without PDF convolution) would also be accessible at a

lepton collider, since this signal channel is indifferent to the SUSY production mechanism.

When looking at the full event, with SUSY production and the full decay, with such a small decay width, MadEvent fails to sample an appropriate phase space and the results of the Monte Carlo integration are unreliable. This can be illustrated as follows: in the narrow-width approximation,

$$d\sigma_{tot} = d\sigma_{prod}\frac{\Gamma_{decay1}}{\Gamma_{total}}\frac{\Gamma_{decay2}}{\Gamma_{total}} \tag{7}$$

where here BR$= \Gamma_{decay1/decay2}/\Gamma_{total} \sim 1$ for both decays and a very narrow neutralino decay width $\Gamma_{total}/m_{\tilde{\chi}_1^0} \ll 1$, the cross section of neutralino pairs should be the same, regardless of whether or not their decays are included, that is $d\sigma_{tot} = d\sigma_{prod}$, which is not found with MadEvent when including the neutralino decays in this model. The way evchain circumvents this limitation is in a way by implementing the narrow-width approximation "by hand". The production process for neutralinos is done in one run of MadGraph (either by direct pair production or via any SUSY cascade) and the decay of the neutralinos is done in another, separate run. The resulting LHE event files from these two separate runs are combined by evchain (with the appropriate Lorentz boosts being made), and the cross section calculated from production events is scaled by the branching fraction to the decay events, as per the narrow width approximation of Eq. 7. In the case of the axino LSP, no scaling is necessary since the branching is effectively one, but when similar events with gravitinos and RPV decays are generated for comparison, the appropriate scaling has to be applied.

A minimal set of loose default generation cuts are implemented in MadEvent (with any other cuts done during the analysis). These cuts include a minimum jet p_T of 1 GeV, a minimum invariant mass between any pair of jets of 1 GeV and a delta R between jets of 0.1 This set of cuts is the same for all three models (axino/gravitino/RPV). It should be noted that these cuts themselves, are "boosted" by evchain as well, for example a small minimum p_T requirement on a jet will actually cut events at a higher p_T after evchain boosts the events. This effect should be negligible however, as in all the events generated the p_T of jets is rather large (also good news for triggering) because of the mass of the neutralino NLSP.

The comparison models are intended to be as similar as possible to the benchmark cases for axinos so that distinguishing between events here can be thought of as a "worst case" scenario, where distinguishing models is the most difficult. This also means that the axino is taken to be very light, like the gravitinos or neutrinos (from RPV) that appear in the

alternative neutralino decays. A heavier axino will provide more handles for distinguishing neutralino decays via the kinematic distributions. Of course the ability to distinguish between distributions is dependent on the ability of the detector to measure such features when the jets are highly displaced, and again, no detailed detector simulation is attempted in this work. Aside from the axino mass and the gravitino mass, the rest of the SUSY spectra is identical between the models, so the production rates above are the same for all three alternatives (axino/gravitino/RPV). In addition to the similar spectra, the width of the lightest neutralino to 2 jets and MET is made to be very close to the axino benchmarks so that the similar signal would appear in the same region of the detector (though not necessarily at the same rate, since the total width does not have to be the same as the axino benchmark). It is reasonable to assume that other comparison models could produce better "imposter" signals, by having a higher rate (from a different SUSY spectra) and a different decay length, but with a comparable number of events in the same part of the detector. Comparison of the axino benchmark signal to these two comparison models follows, with gravitinos first, and then with the RPV signal.

In the case of gravitinos, to have a neutralino decay length for the 2 jet and MET signal similar to the axino model, the gravitino mass is taken to be 500 eV for the lighter benchmark and 750 eV for the heavier one. Unlike the axino, the gravitino has numerous couplings, and is not restricted to the 2 jet+MET channel. One obvious consequence of this is that gravitinos can be distinguished from axinos simply by looking for these other decay channels, e.g. anything with leptons or photons that is highly displaced. There is plenty of literature describing how to search for gravitinos with leptons or photons, see, e. g., [43], but this is not enough to rule out the possibility that some of the displaced multi-jet signal could be coming from axinos. While it would require a coincidence of parameters, neutralino decays to gravitinos and axinos could co-exist in a model, so for the sake of being thorough, the 2 jet+MET signals can be compared in hopes of distinguishing them based on the shapes of kinematic distributions alone. By the same reasoning, the presence of alternative decay channels for the gravitino means that the branching fraction will be less than one, and so for identical SUSY spectra the gravitino model will have the multi-jet+MET signal occurring at a smaller rate. Unlike the axino case, there are several topologies to produce two jets and a gravitino (see Figure 7). While the same topology exists as in the axino case (Figure 7 left), it is not dominate here, as there are also topologies without off-shell colored sparticles

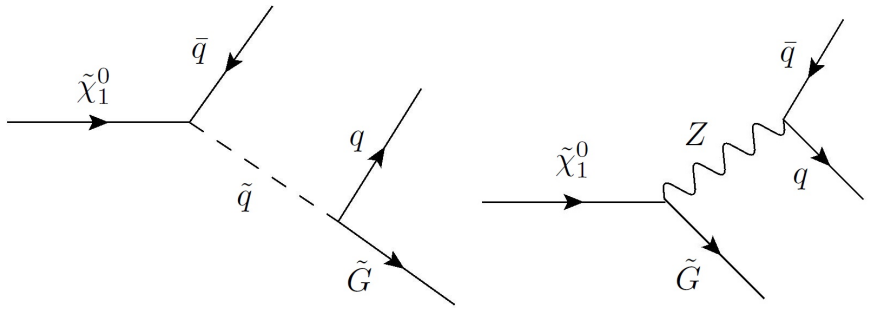

FIG. 7: Two diagrams that contribute to neutralinos decaying to two jets and a gravitino.

that contribute with much more strength (Figure 7 right). Diagrams like the right one in Figure 7 give two hints as to how the scenarios can be distinguished. Since the dominant topology has the gravitino radiated at the beginning of the decay chain, rather than the end, we should expect the MET to recoil differently between the axino and gravitino models, with the gravitino MET being harder. Conversely, the visible jets should be harder for the axino case, and softer for the decays to gravitinos. These kinematic differences are subtle when looking at neutralino decays for this particular benchmark, and when these decays are simulated for a SUSY cascade the effect is washed out by the boosts and smearing by the PDFs. For a model with a much heavier neutralino this difference is more noticeable. Results comparing the MET for axino events versus gravitino events are shown in Figure 8 and results comparing the total jet p_T (the H_T) are shown in Figure 9. Jet p_T and MET being relatively larger or smaller between decays with axinos or gravitinos is not a very useful handle by itself. If only one type of decay is actually measured, it begs the questions: more or less p_T compared to what? The difference in weighting between visible and invisible p_T can be seen by plotting H_T against the MET, as shown in Figure 10. In all of these kinematic plots the effect is more noticeable for larger neutralino masses, but it is still smeared away in the full event, i. e. when including both production and neutralino decays.

Perhaps a simpler way to distinguish these two models is to just count the displaced jets. It is reasonable to think that after parton showering with Pythia and clustering we could expect more jets from the axino case as these jets are expected to be harder (based on the kinematic distributions above) and are more likely to radiate, and this is reflected in the generated events as shown in Figure 11. Applying stronger jet p_T cuts to satisfy triggers [60] ($p_T > 40$GeV) will remove the softer jets from both samples, in addition to a pseudo-rapidity cut ($|\eta| < 2.5$). This does not just reduce the total number of jets after showering, but it

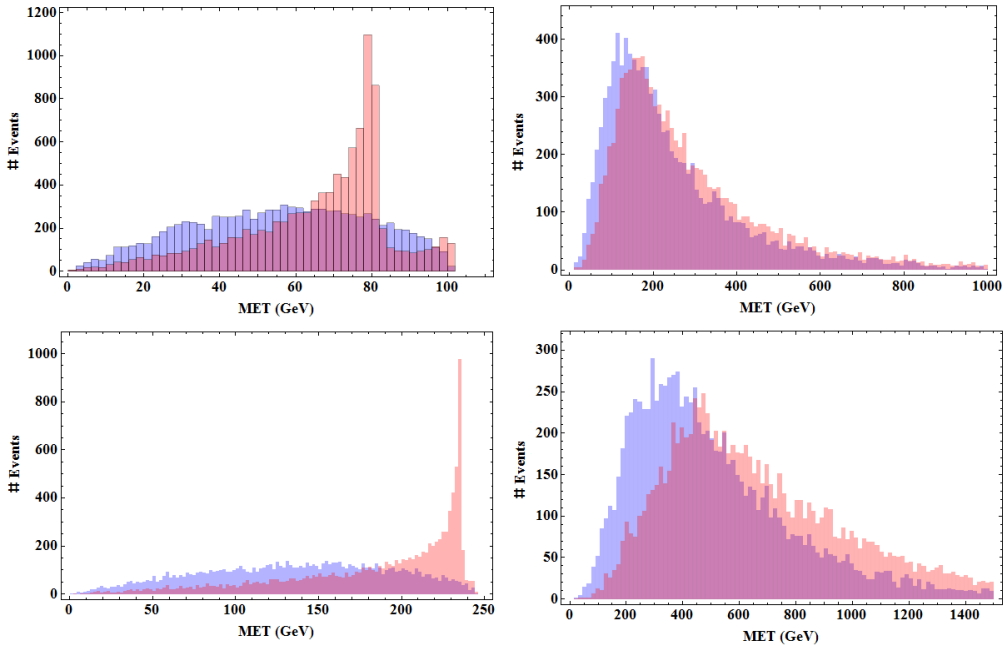

FIG. 8: Distributions of the MET from neutralino decays to axinos (blue) and gravitinos (red). Events are simulated with minimal generation cuts only, and at parton level (no showering/clustering). The left plots consider the neutralino decay alone, while the right plots are in the lab frame of the whole event at 14 TeV at the LHC, i.e. when including both production and decay via evchain. The upper plots are for the lighter benchmark, and the lower plots for the heavier benchmark.

also shifts events between different bins for numbers of jets.

Even though a photon or a Higgs boson could take its place in diagrams similar to the left diagram in Figure 7, the presence of the s-channel Z has a significant effect on the distributions and the Z resonance can be reconstructed. For event samples from just the decays, the Z resonance simply comes from the invariant mass of both jets (Figure 12). When looking at the full event with showering there is the question of which jet combination to take. Including the full combinatoric background (all combinations of jets), the Z resonance is buried, but since the particular resonance is known in this case, it is easy enough to just take those combinations of jets which are closest to the known Z mass. This method has the draw back that it can create an artificial bump in the jet invariant mass distribution. This artificial bump is much more pronounced when the parent neutralino is lighter, so again, like the other methods of discrimination, it is more difficult for lighter neutralinos.

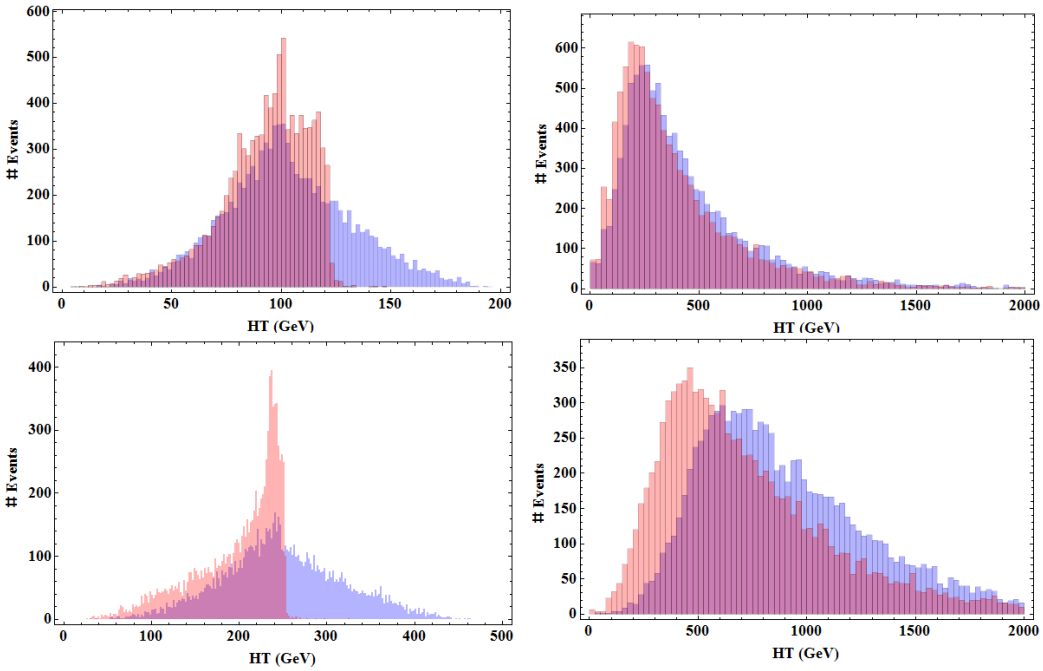

FIG. 9: Distributions of the scalar sum of jet transverse momenta (the H_T) from neutralino decays to axinos (blue) and gravitinos (red). Events are simulated with minimal generation cuts only, and at parton level (no showering/clustering). The left plots consider the neutralino decay alone, while the right plots are in the lab frame of the whole event at 14 TeV at the LHC, i.e. when including both production and decay via evchain. The upper plots are for the lighter benchmark, and the lower plots for the heavier benchmark.

Reconstructing the Z resonance is a much more powerful way to distinguish the gravitino and axino cases, as unlike the kinematic distributions discussed earlier it is invariant to boosts and somewhat insensitive to the sparticle masses. A veto on the invariant mass of jet pairs in separate halves of the detector (pairs from separate parent neutralinos) can cut the majority of gravitino events and of the methods described here such a veto is considered the best way to determine if neutralino decays contain events with axinos, gravitinos, or both.

Like gravitinos, RPV scenarios can also produce a signal of displaced jets and missing energy, and RPV decays can co-exist in a model with decays to axinos, so a comparison of these similar signals is warranted. There are many possible signatures of RPV as there are several possible couplings, coming from both the super potential and also from soft SUSY

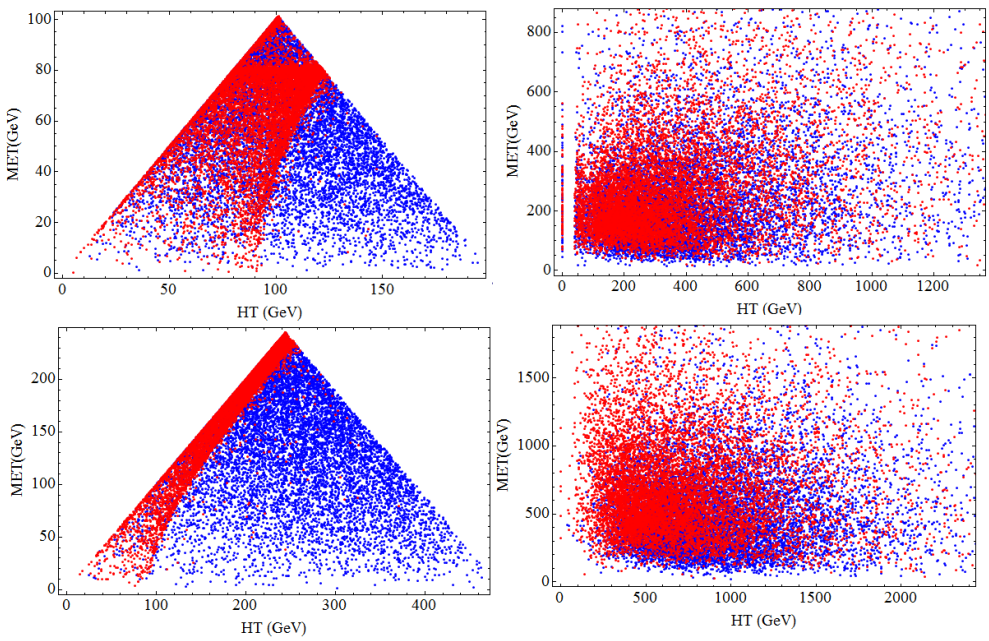

FIG. 10: H_T versus MET from neutralino decays to axinos (blue) and gravitinos (red). Events are simulated with minimal generation cuts only, and at parton level (no showering/clustering). The left plots consider the neutralino decay alone, while the right plots are in the lab frame of the whole event at 14 TeV at the LHC, i.e. when including both production and decay via evchain. The upper plots are for the lighter benchmark, and the lower plots for the heavier benchmark.

breaking terms. The couplings from the R-parity violating super potential are given by [79]

$$W_{RPV} = \mu_i H_u L_i + \frac{1}{2}\lambda_{ijk} L^i_L \cdot L^j_L E^k_R + \lambda'_{ijk} L^i_L \cdot Q^{jl}_L D^k_{Rl} + \frac{1}{2}\lambda''_{ijk}\epsilon^{lmn} U^i_{Rl} D^j_{Rm} D^k_{Rn} \ ,$$

where i, j, k are flavor indices and l, m, n are color indices. The first three terms all violate lepton number, while the last term violates baryon number. While all these couplings are possible, they are constrained by the non-observation of certain processes. To avoid running into bounds from unobserved processes, such as proton decay, the constraint is not on the size of these couplings directly, but rather of their products (for example proton decay requires B and L to be violated). Because of this it is not unreasonable to assume that there could be just one dominate RPV coupling, that is itself relatively small. The UDD coupling can produce three displaced jets from neutralino decay (Figure IV), which may look like the axino signal after showering/clustering but any missing energy would have to come from detector/trigger inefficiencies, or jet mis-measurement. It is difficult to estimate

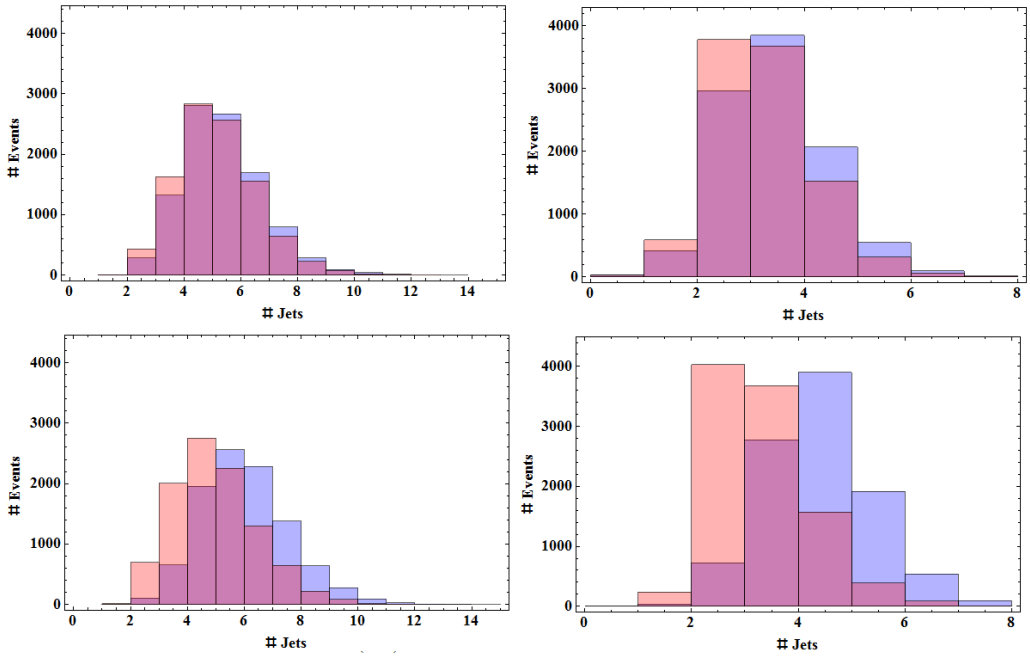

FIG. 11: The number of jets from neutralino decays to axinos (blue) and gravitinos (red). All plots are for the full event (production and decay via evchain) at 14 TeV with showering done by PYTHIA and jet clustering from FastJet using k_T jets with $D = 0.4$. The left plots are from events generated with loose generation cuts and the right plots are obtained after applying more restrictive cuts, $p_T > 40$ GeV and $|\eta| < 2.5$. The upper plots are for the lighter benchmark, and the lower plots for the heavier benchmark.

how much "fake MET" there could be in such events without performing a detailed detector simulation, but it is expected that such events would be distinguishable from axino events for any model similar to the benchmarks, because the NLSP neutralinos are massive enough and the axino will carry away a large portion of this energy, as shown in the MET plots in Figure 8. Also, due to the absence of true MET the jets themselves will be harder than in the axino case.

In the case where the dominant RPV coupling is of the LQD type (with $\lambda' \approx 7.5 \times 10^{-6}$ for the lighter benchmark and $\lambda' \approx 2.5 \times 10^{-6}$ for the heavier benchmark), the two jet signal can look very much like the axino case when the neutralino decays to two jets and a neutrino. As in the gravitino case, this RPV coupling also allows for channels with photons and charged leptons in the final state. Again, the presence of other channels will mean the rate of the 2

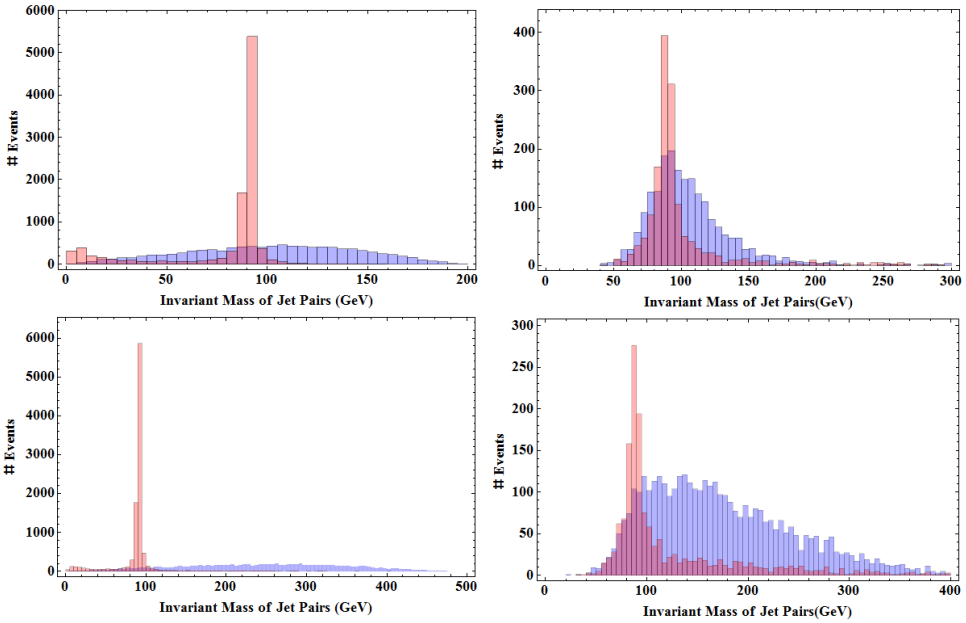

FIG. 12: The invariant mass of jet pairs for neutralino decays to axinos (blue) and gravitinos (red). The left plots are for a single decaying neutralino in its rest frame, while the right is in the lab frame for the whole event (in a sample selected to have exactly four jets) at 14 TeV with showering done by PYTHIA and jet clustering from FastJet using k_T jets with $D = 0.4$. The upper plots are for the lighter benchmark, and the lower plots for the heavier benchmark.

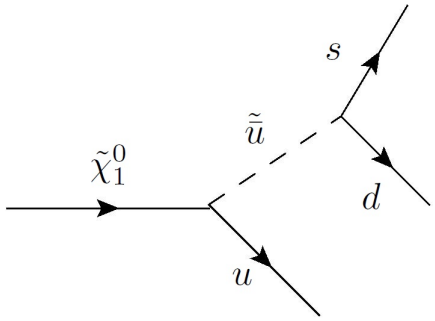

FIG. 13: RPV topology with UDD coupling.

jet signal is less than in the axino case, but a difference of rates is not helpful without a priori knowledge of the SUSY spectra to calculate these rates . Discovery of displaced photon or charged channels would imply there are neutralino decays not involving the axino, but again, as was mentioned with the gravitino case, this does not exclude the possibility that both decays exist in the same model. While it was stated that it would require a coincidence of parameters to have competitive neutralino decays to gravitinos and axinos in the same model,

it would be less surprising in the case of RPV with trilinear couplings, such as the UDD or LQD ones explored here. Affleck-Dine baryogenesis (ADB) with RPV couplings [80] is a scenario that is attractively compatible with a cosmology with LSP axinos in the hadronic axion window. This is because with such a low Peccei-Quinn scale, f_a, the scenario likely requires a very low reheating temperature, (which ADB can accommodate, unlike thermal Leptogenesis). Also, when ADB involves RPV couplings, there must be another source of dark matter instead of the lightest neutralino, which axions/axinos can accommodate. The coincidence of scales required to make both RPV and axino decays competitive comes from two independent sources. For the axinos, the window of lower f_a is set by the constraints mentioned in Section II, and for ADB with RPV to be successful it requires a trilinear RPV coupling with $\lambda \approx 10^{-7}$[80], coincidentally in the same range to give similar width as the axino decays. Though it is a distinct possibility that these channels co-exist in the same model, the "coincidence" should not be overstated, as depending on the value of f_a the width to axinos actual varies over a couple orders of magnitude, and with RPV, ADB can be accommodated with $10^{-9} < \lambda < 10^{-6}$, so while these correspond to the same range of widths for decays, it is also possible that one process dominates and the other will have a negligible rate.

Distinguishing LQD RPV from axino signals by the jet distributions alone is much more difficult than the case with gravitinos as the topologies contributing to the signal are now identical (Figure 14). There is no massive resonance to distinguish the models as in the case of gravitinos, and the MET and various jet variables are also very similar between this case and the axino case. Some of the distributions explored earlier are shown again in Figure 15, but now with LQD RPV distributions as well. The only one that could potentially be used as a tool to distinguish axino and RPV signals is the H_T, which shows a peak at half the parent neutralino's mass for the axino case, but not for the RPV case. This is only useful if the neutralino mass is known or at least constrained (perhaps from analysis of the prompt event separately) and the distribution is only useful in the neutralino rest frame, so its momentum must also be determined. If sufficiently long lived RPV decays are discovered at the LHC, it may be very difficult to rule out the possibility of a light axino contributing to some of that signal.

When considered together, there are a few handles to distinguish between gravitino and axino scenarios, and with varying success, some RPV scenarios, but it should also be asked

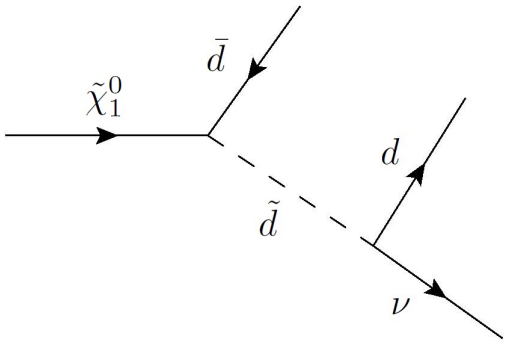

FIG. 14: RPV topologies with LQD coupling.

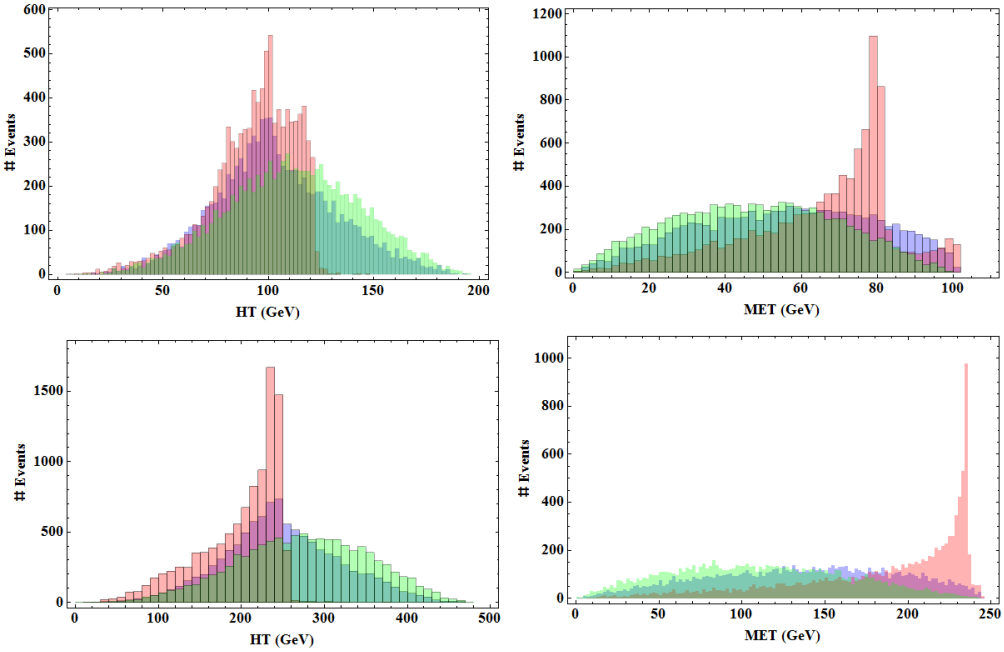

FIG. 15: Summary of kinematic distributions for all three scenarios, axino (blue), gravitino (red) and RPV with an LQD type coupling (green). Events are simulated for the decay only with minimal generation cuts only, and at parton level (no showering/clustering). The top row is the lighter benchmark and the bottom row is the heavier benchmark.

how strongly any of these results depend on the choice of benchmark. Most of the distinguishing features above come about simply as a consequence of the topology, and should not be very sensitive to many aspects of the benchmark. The parameter that is expected to have the greatest effect on the shapes of these distributions is the mass of the lightest neutralino, which has been demonstrated in our results for the kinematic distributions. The

choice of neutralino mixing, in this case a mostly Bino NLSP, does not have a large effect on any of the axino distributions shown here, and the largest effect this has on the gravitino signal is to change the branching ratio to jets, but the rates are already very different from the axino case.

The more important effect from varying the SUSY mass spectra and mixings is in how it affects the width. The determination of the effect of the neutralino mixing on the width is straight forward when looking at the Feynman rules for diagrams like those in Figure 2 and 4. In both cases, the neutralino decay chain begins with an off-shell squark, but only the wino and bino components of the neutralino will couple to the squark. The smaller these components, the smaller the total width will become. In the following we will study in more detail the decay width for $\tilde{\chi}_1^0 \to q\bar{q}\tilde{a}$.

Overall, we found that the KSVZ axino in the window of smaller f_a has a rather predictive signal. The multiple displaced jets and missing energy signature is not unique, but can at least in principal be distinguished from the more well studied alternatives for neutralino decays and the signal is not particularly sensitive to the choice of the PMSSM benchmark model.

A. The decay width for $\tilde{\chi}_j^0 \to q\bar{q}\tilde{a}$

The neutralino decay width of Figure 4 for massless quarks and with universal squark masses $m_{\tilde{q}} = m_{\tilde{q}_L} = m_{\tilde{q}_R}$ is given by [68]

$$\begin{aligned}\Gamma(\tilde{\chi}_j^0 \to q\bar{q}\tilde{a}) \;=\; & \frac{m_{\chi_j^0}\alpha g_{\rm eff}^2}{64\pi^2 \sin^2\theta_w}\frac{3}{2}\sum_q 16[(T_{3q}Z_{j2} + (Q_q - T_{3q})Z_{j1}\tan\theta_w)^2 + Q_q^2 Z_{j1}^2\tan^2\theta_w] \\ & \times\; [g(m_{\tilde{a}}^2/m_{\tilde{\chi}_j^0}^2, m_{\tilde{q}}^2/m_{\tilde{\chi}_j^0}^2) + h(m_{\tilde{a}}^2/m_{\tilde{\chi}_j^0}^2, m_{\tilde{q}}^2/m_{\tilde{\chi}_j^0}^2)]\;, \end{aligned} \tag{8}$$

where Z_{ji} are the matrix elements of the matrix which diagonalizes the neutralino mass matrix, θ_w is the weak mixing angle, and $Q_q = (2/3, -1/3), T_{3q} = (1/2, -1/2)$ for (up,down)-type quarks. The effective coupling g_{eff} is given by Eq. 6 and the functions g, h are provided in [68].

It was emphasized in Section III that the displaced multi-jet and MET signal was the only one that need be considered for decays to axinos, but one can imagine that with the lightest neutralino as a sufficiently pure Higgsino that diagrams like in Figures 2 and 4 would be suppressed enough that another decay channel can dominate. While other axino channels

can have a larger partial width than the 2 and 3 jet channels for a very pure Higgsino, these channels are still very much suppressed themselves, as they will contain additional final-state particles or additional off-shell sparticles or both. This possibility was explored for the lighter benchmark only by varying the mixing parameters and retaining the same mass spectrum. For this benchmark case the alternative channels, containing additional gauge bosons or a Higgs boson only began to become competitive with the multi-jet channels once the decay length was already several orders of magnitude outside of the detector (hundreds of kilometers instead of meters). Even though this possibility was only explored for a single benchmark, it seems unlikely that any choice of spectra could reduce the decay length by enough that it would matter to the phenomenology. The effect of varying the Peccei-Quinn scale f_a over the allowed window is also relatively straight-forward (see Eq. 8). How exactly the neutralino width scales with f_a will depend on which of the two couplings is dominant, but in either case the width will vary by about two orders of magnitude.

The other parameters affecting the width are all sparticle masses: The axino mass, the neutralino mass, the squark mass and the gluino mass. In Section III it was stated that several of the Snowmass PMSSM benchmarks from the collection in [61] allowed for neutralino decays to axinos with a decay length appropriate for searches at the LHC, even though only two were chosen for simulation, and it seems as though this scenario could be rather common for SUSY models with sparticle masses in the range that is explorable in the near future. With the decay width of neutralinos to axinos depending on so many variables it is difficult to bound exactly what the model space is available to such searches, but Figures 16 through 19 make an attempt of demonstrating what range of SUSY parameters would allow for this type of signal. Each is a plane in parameter space that shows contours of equal neutralino decay length $c\tau$ for the 2 jet plus axino signal only, as given in Eq. 8. For very heavy neutralinos the channel to heavy quarks opens up, and for squarks much heavier than gluinos the 3 jet signal will start to become competitive and eventually dominate. In each of these plots the neutralino is taken to be a very pure bino and the Peccei-Quinn scale f_a takes its lowest value in the allowed window, so that these planes of parameters space are already at there "least displaced" for these parameters. These plots also show for what SUSY masses prompt decays to axinos may be possible, though this signal comes with its own set of challenges that are not discussed here.

A compressed spectrum (with a neutralino NLSP mass close to the gluino mass) will make

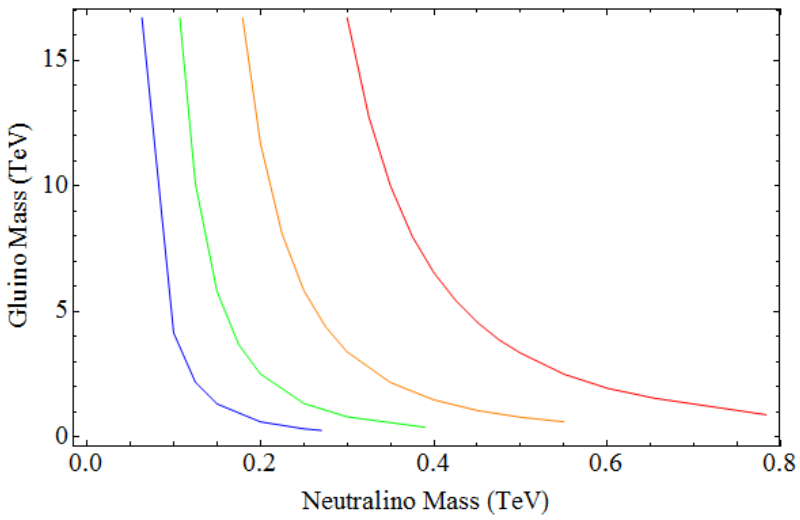

FIG. 16: Contours of constant neutralino decay length $c\tau$ for decays to an axino and two jets. Red is 0.01 m, yellow is 0.1 m, green is 1 m and blue is 10 m. All squarks are at 2 TeV and the axino is taken to be massless.

the off-shell decay to axinos easier, resulting in a shorter mean decay length. The spectra can become very compressed and the decay will still be displaced, (especially for larger values of f_a), perhaps providing an easier discovery channel than otherwise available for a compressed spectrum. For less compressed spectra, or spectra with a lighter neutralino, the mean decay length increases. When considering a larger parameter space of SUSY models (as the PMSSM does), compressed spectra are not uncommon [81]. While more compressed spectra can be very difficult to search for at colliders [82], in this case the primary effect on the signal is on the total width of the NLSP, and typically more compressed spectra will simply have the displaced jets closer to the primary vertex (with some fraction still being more displaced). This is an interesting scenario in and of itself, implying that an otherwise difficult to study spectrum at the LHC may have axino production as its discovery channel.

V. DARK MATTER ABUNDANCES IN THE HADRONIC AXION WINDOW

There are also many unanswered questions concerning the cosmology of such a model. In this work, we only attempt to argue that there are enough parameters that can be adjusted and that such a model has all the right ingredients for a working cosmology, but this does

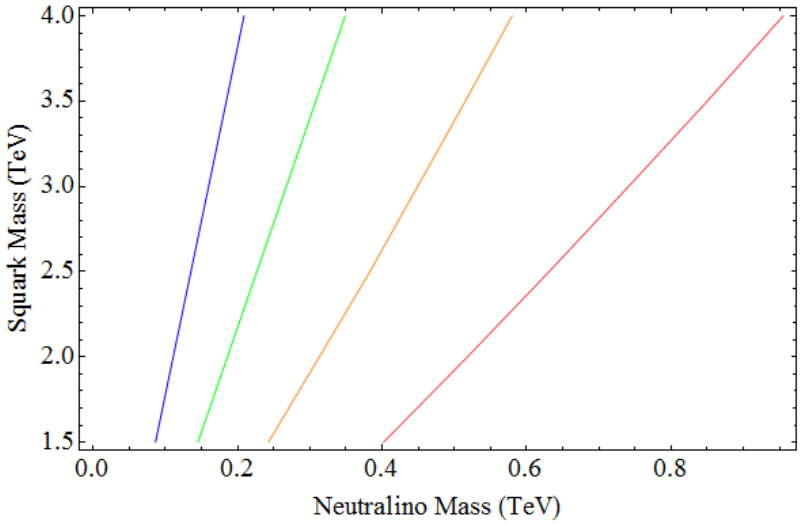

FIG. 17: Contours of constant neutralino decay length $c\tau$ for decays to an axino and two jets. Red is 0.01m, yellow is 0.1m, green is 1m and blue is 10m. The gluino mass here is 3 TeV and the axino is taken to be massless.

not guarantee such a cosmology exists. It seems as though a low reheating temperature (T_{rh}) is required to make this scenario viable. With a reheating temperature lower than the freeze out temperature (T_F) for axions, constraints from large scale structure and CMB measurements can be avoided and the hadronic axion window is still viable [56]. The size of axion and axino DM abundances depends on a number of factors that have not been specified here because they do not effect the collider signal. The phenomenology here is relatively insensitive to the axino mass, which will effect the size of its abundance and how relativistic it is. Late decays of the saxion can effect the size of both the axion and axino population, and can inject extra entropy into the early universe to dilute these species, so the role of the saxion is non trivial and requires further study in this scenario. The gravitino was assumed to be heavy enough not to effect the collider phenomenology in this scenario, but it too could play a more complicated role. A light enough gravitino can have a comparable coupling with the LOSP as the axino (as shown in Section IV), but can also be coupled more strongly or weakly depending on its mass. While only an LSP gravitino is likely to impact the collider phenomenology discussed here, an intermediate mass gravitino can still effect the cosmology with late decays to other states. Whether or not there are RPV couplings present can also effect both the axino and axion abundance. There are several options for

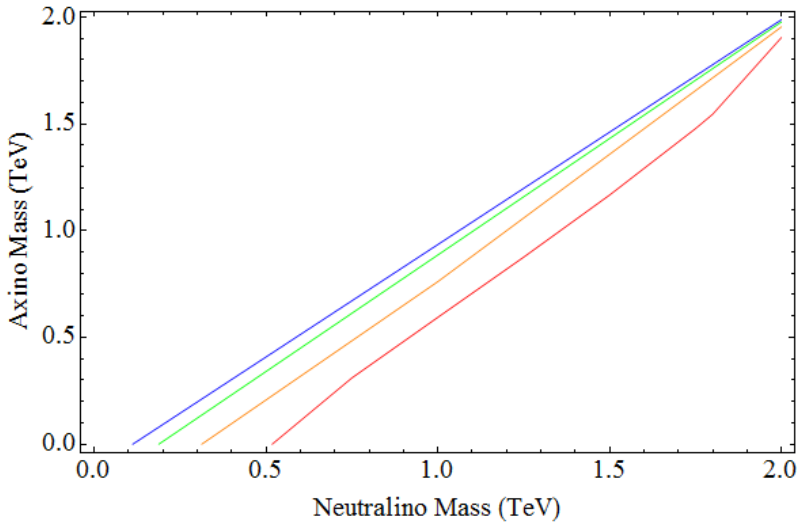

FIG. 18: Contours of constant neutralino decay length $c\tau$ for decays to an axino and two jets. Red is 0.01m, yellow is 0.1m, green is 1m and blue is 10m. The gluino mass here is 3 TeV and all squark masses are at 2 TeV.

what types of RPV couplings there are (if any) and the size of each coupling has a wide allowed range. The axion/axino cosmology is more sensitive to the choice of RPV couplings in this case, because the axion/axino couplings are restricted in the hadronic axion window, and so there are not as many options for decay chains.

With so many possible variables, we only attempt to illustrate the viability of such a scenario in the simplest case, i.e. with no RPV and ignoring the possible effects of gravitinos and saxions. In this case there are still several possible populations of DM: thermal and non-thermal relics from both axions and axinos.

For $f_a > T_{rh}$ the contribution from non-thermal axions to the cold relic abundance from the misalignment mechanism is approximated by [83] (for a review see, e.g., [84]):

$$\Omega_a^{NTP} h^2 \approx 0.15 \xi f(\theta_i^2) \theta_i^2 \left(\frac{f_a}{10^{12} GeV} \right)^{7/6} \tag{9}$$

with $\xi = \mathcal{O}(1)$ parameterizing theoretical uncertainties, θ_i denoting the misalignment angle with respect to the CP-conserving position, and $f(\theta_i^2)$ accounts for anharmonic corrections due to large values of θ_i ($f(\theta_i^2) \approx 1.2$ [83]). Even when assuming $|\theta_i| = \pi$ this contribution from non-thermal axions to the CDM abundance is negligible for f_a in the hadronic window.

The thermal axion abundance at very low reheating temperatures is calculated numeri-

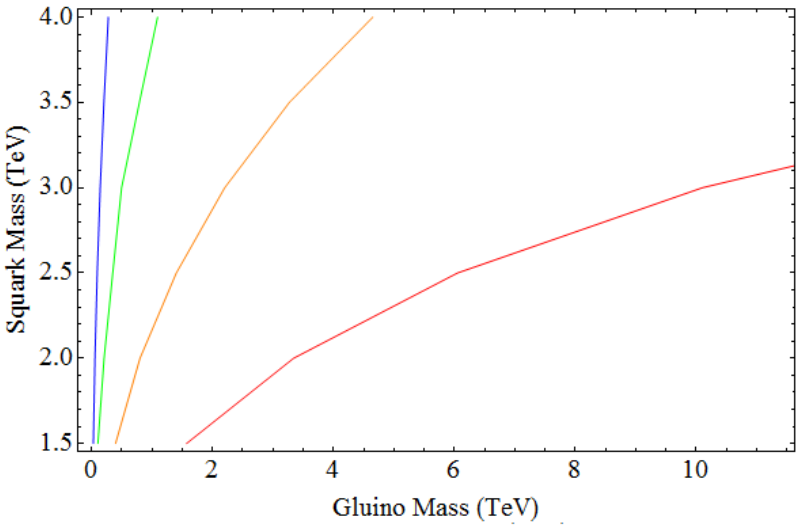

FIG. 19: Contours of constant neutralino decay length $c\tau$ for decays to an axino and two jets. Red is 0.01m, yellow is 0.1m, green is 1m and blue is 10m. The neutralino mass here is 0.5TeV and the axino is taken to be massless.

cally in [56]. Using that the axion mass m_a is related to the PQ scale f_a as [41]

$$f_a = \frac{\sqrt{z}}{1+z}\frac{f_\pi m_\pi}{m_a} \approx \frac{6\times 10^6 \text{eV GeV}}{m_a(\text{in eV})} \tag{10}$$

we use the results for $\Omega_a/\Omega_0(T_{rh})$ provided in Figure 4 of [56] for 5eV $\leq$ m$_a$ $\leq$ 20 eV (corresponding to 3×10^5GeV $\leq f_a \leq 1.2\times 10^6$ GeV) to estimate $\Omega_a h^2$ for the hadronic window for f_a. We assume $\Omega_0 h^2 = m_a/13\text{eV}/g_{*S,F}$ with the effective number of relativistic degrees of freedom $g_{*S,F}\approx 10$ at freeze-out temperature $10\,\text{MeV} < T_F < 100$ MeV [85]. The resulting thermal axion abundance as a function of reheating temperature T_{rh} is plotted in red in Figure 20 for $f_a = 3\times 10^5$GeV and $f_a = 1.2\times 10^6$ GeV. Axion constraints are completely lifted in the lower range of T_{rh} shown, but rising towards 50 MeV, the constraints may become relevant again with a dependence on f_a (see [56]).

The other possible major component expected is the thermal abundance of axinos. With a lower f_a scale one may expect the thermal axinos to over-close the universe, but they too will be diluted due to a lower reheating temperature. An approximation of this dilution is given in [86], which may be used to rescale the abundance at high T_{rh} down to its value in the low reheating scenario:

$$\Omega_{DM}h^2 \approx \left(\frac{T_{rh}}{m_\chi}\right)^3 \left(\frac{m_\chi}{T_F}\right)^3 \Omega_{DM}h^2(\text{High}T_{rh})\,. \tag{11}$$

The thermal axino abundance for a sufficiently large reheating temperature is given by [22]:

$$\Omega_{\tilde{a}} h^2 = \frac{m_{\tilde{a}}}{2KeV} \,. \tag{12}$$

Thermal axino production at low reheating temperatures was explored in more detail in [87], but only down to reheating temperatures as low as 1 GeV. At even lower temperatures axinos become decoupled from kinetic equilibrium but still remain in chemical equilibrium. For a treatment of this scenario, we follow the methodology of [88], which originally studied goldstino production at low reheating temperature, but can be applied to axinos by adjusting the corresponding couplings. At lower reheating temperatures axinos freeze out earlier, and will be diluted more greatly by entropy produced during inflation. Assuming goldstino production via squark decay described by $\Gamma_{\tilde{q}\to\xi q} = m_{\tilde{q}}^5/(16\pi^2 F_\xi^2)$, the freeze out temperature in this scenario is determined in [88] from:

$$3H(T_F) = 1.4(5\pi^2 g_*/72)^{1/2} \frac{T_F^4}{M_P T_R^2} \simeq \frac{12 m_{\tilde{q}}^5}{16\pi F_\xi^2} \sqrt{\pi} \left(\frac{m_{\tilde{q}}}{T_F}\right)^{3/2} e^{-m_{\tilde{q}}/T_F} \,. \tag{13}$$

In [57] the decay width for axino production via $\tilde{q} \to q\tilde{a}$ is given as $\Gamma_{\tilde{q}\to\tilde{a}q} = g_{eff}^2 m_{\tilde{q}}/(16\pi^2)$ with g_{eff} of Eq. 6, so that the freeze out temperature can be determined from Eq. 13 by replacing F_ξ accordingly:

$$F_\xi \to \frac{m_{\tilde{q}}^2}{g_{eff}} \,. \tag{14}$$

The resulting dependence of the reheating temperature on the freeze out temperature is shown in Fig. 21, for an example case at $f_a = 3 \times 10^5$GeV with squarks and gluinos with masses 1 and 2 TeV respectively. As the reheating temperature approaches the low values necessary to avoid axion constraints, the freeze out temperature gets larger very quickly, and it is the ratio of these two scales which will determine how diluted the thermal abundance is. Using the reheating and freeze out temperatures from Fig. 21 and the more accurate method of [88] with F_ξ adjusted as in Eq. 14, we find the relic abundance to be many orders of magnitude below the amount observed today for the range of axion masses considered here ($\Omega_{\tilde{a}} h^2 \approx 10^{-5} m_{\tilde{a}}/\text{GeV}$). To be able to obtain the abundance for $T_{rh} < 100$ MeV from the method used in [88] would require a re-evaluation of the approximations used in the calculation, which is beyond the scope of this work, but the expected effect of going to even lower reheat temperature is to have a thermal axino abundance even smaller than this already negligible amount.

There is also the possibility of a non-thermal axino abundance, from the decays of neutralinos, but its number density is effectively diluted twice. Before considering the diluting effects of going to a very low reheating temperature, the number density of non-thermal axinos is inherited from neutralinos but scaled by the ratio of masses,

$$\Omega_{\tilde{a}}^{NTP} h^2 = \frac{m_{\tilde{a}}}{m_{\tilde{\chi}_1^0}} \Omega_{\tilde{\chi}_1^0} h^2. \tag{15}$$

For a reasonable range of axino masses (between MeV and a few GeV), this already results in a large reduction of the non-thermal axino abundance. On top of this, $\Omega_{\tilde{\chi}_1^0} h^2$ must be rescaled for a very low reheating temperature, since the neutralino number density itself would also have been diluted away during inflation. Even for SUSY spectra that grossly overproduce bino NLSPs at high T_{rh}, ($\Omega_{\tilde{\chi}_1^0} h^2(\text{High} T_{rh}) > 10^5$), the neutralino relic abundance (and by extension the non-thermal axino abundance) is usually negligible for reheating temperatures small enough to avoid axion constraints ($T_{rh} < 100$ MeV). Only when both the neutralino abundance and the axino mass are very large, the non-thermal axino component may be sizable. Axinos in this mass range (approaching the neutralino mass) are unlike those in the benchmarks whose phenomenology is studied here (where axinos were considered light), but heavier axinos should be easier to distinguish from similar decays with gravitinos or with RPV. The most likely scenario then seems to be a dark matter abundance that is mostly thermally produced axions, but with the possibility of a significant fraction being non-thermal axinos, if they are heavy enough (compared to the neutralino mass). If these two populations do not saturate the relic abundance there is also the possibility of inflaton decays directly to axinos, which would provide an additional component, but this is highly model dependent. This is just one possible scenario, without considering gravitinos, saxions or RPV, but it should evade all existing constraints and such a model will have a collider signal that is very similar to the signal discussed in this work.

VI. CONCLUSIONS

Supersymmetric models with axions and axinos are very attractive extensions of the SM since they can address issues of naturalness in QCD, in the electroweak sector, and with regards to dark matter. The one feature of these types of models that could be considered disappointing is that the additional particles, the axion and the axino, can be rather difficult

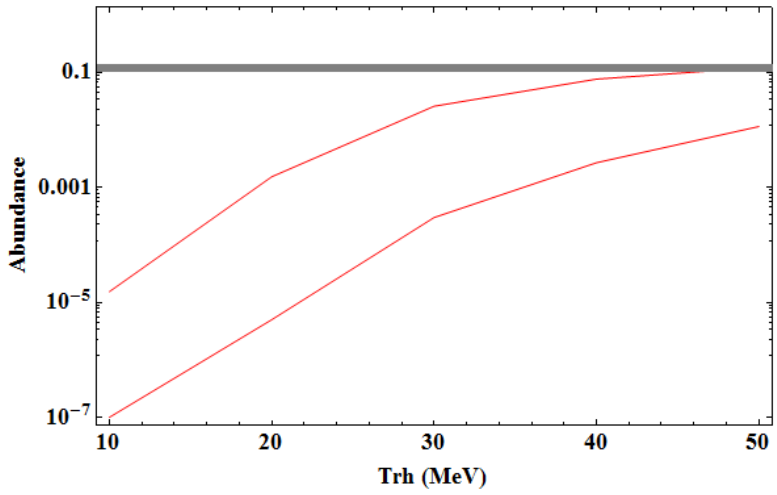

FIG. 20: The thermal relic abundance of axions as a function of reheating temperature. Two curves are shown, as the scale f_a (or equivalently the axion mass m_a) is varied over its possible values within the hadronic axion window. The approximate measured value of the total dark matter relic abundance is shown by the solid gray line ($\Omega_{DM}h^2 = 0.119$)[89].

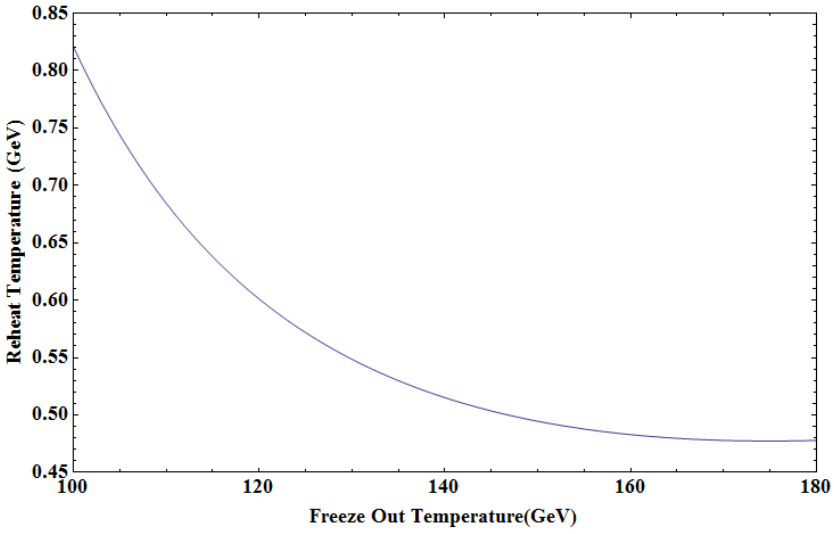

FIG. 21: The reheating temperature vs the freeze out temperature for the scenario of thermal axino production at low reheating temperature for an example case at $f_a = 3 \times 10^5$GeV with squarks and gluinos with masses 1 and 2 TeV respectively. At lower reheating temperatures axinos will freeze out sooner, and be diluted more severely.

to detect. The scenario proposed here is a PQMSSM model with a light LSP axino with only QCD couplings and a neutralino NLSP. The signal studied here is the production of neutralinos and their displaced decay to two jets and a KSVZ axino via an effective squark-quark-axino coupling. This scenario could be detectable at the 14 TeV LHC provided the Peccei-Quinn scale can exist in the smaller range $3 \times 10^5\,\text{GeV} < f_a < 3 \times 10^6\,\text{GeV}$ (hadronic axino window). We did not consider sneutrino NLSPs, in which case the topologies for NLSP decays becomes more varied and can include photons and charged leptons, making the phenomenology more complicated, especially in distinguishing from RPV and gravitino scenarios.

The scenario of the hadronic axion window is not new, and its cosmology has been discussed in the literature (see, e.g., [54]) but the consequences of having this window in a SUSY model have not been explored until recently, and there is still much to learn. This is not the only scenario that allows axinos to be detectable at colliders, but to the authors' best knowledge it is the only way currently proposed to detect KSVZ axinos with a neutral NLSP. This scenario gives a predictive collider signature due to its limited couplings. We have shown that it has the potential to be distinguishable from similar models with neutralino decay, and that this signature is relatively insensitive to the choices of MSSM parameters. While we find that there is potential for the LHC to be sensitive to the scenario studied here, a detailed detector simulation that implements for instance the triggers used in hidden valley searches [60] is needed to fully assess its observability.

It is interesting to probe the hadronic axion window via collider searches for a variety of reasons. While it has been argued extensively in the literature that there can be a variety of benefits to having SUSY with axions, there are very few ways to test the axion coupling f_a independent of its photon or electron coupling, which this scenario allows for. While there is still much to learn about this scenario, there are tentative hints that it could have attractive features beyond a detectable axino. It may also provide a discovery channel for otherwise difficult to study compressed SUSY spectra, it may alleviate some issues of tuning, and the cosmology it fits in may have other interesting consequences, such as detectable RPV decays that are competitive with decays to axinos. This scenario is still very new, both for collider studies and for cosmology, and much more work is required to determine its viability, detectability and consequences.

Acknowledgments

We thank H. Baer for valuable discussions and comments, and for reading an early version of the manuscript. We also would like to thank Ian Woo Kim for his assistance with evchain and Benjamin Fuks for his assistance with FeynRules. The work of C.S.R. is supported in part by the National Science Foundation under award no. PHY-1118138 and a LHC Theory Initiative Graduate Fellowship, NSF Grant No. PHY-0705682. The work of D.W. is supported in part by the National Science Foundation under award no. PHY-1118138.

---

[1] J. Wess and B. Zumino, Phys. Lett. **B49**, 52 (1974).

[2] J. Wess and B. Zumino, Nucl. Phys. **B70**, 39 (1974).

[3] P. Fayet and S. Ferrara, Phys. Rept. **32**, 249 (1977).

[4] H. P. Nilles, Phys. Rept. **110**, 1 (1984).

[5] H. E. Haber and G. L. Kane, Phys. Rept. **117**, 75 (1985).

[6] S. P. Martin, Adv. Ser. Direct. High Energy Phys. **21**, 1 (2010), hep-ph/9709356.

[7] A. Signer, J.Phys. **G36**, 073002 (2009), 0905.4630.

[8] G. Jungman, M. Kamionkowski, and K. Griest, Phys. Rept. **267**, 195 (1996), hep-ph/9506380.

[9] D. Hooper, C. Kelso, P. Sandick, and W. Xue, Phys. Rev. **D88**, 015010 (2013), 1304.2417.

[10] P. Huang and C. E. M. Wagner, Phys.Rev. **D90**, 015018 (2014), 1404.0392.

[11] H. Baer, V. Barger, P. Huang, D. Mickelson, A. Mustafayev, et al., Phys.Rev. **D87**, 035017 (2013), 1210.3019.

[12] H. Baer, K.-Y. Choi, J. E. Kim, and L. Roszkowski, Phys.Rept. **555**, 1 (2014), 1407.0017.

[13] S. Amsel, K. Freese, and P. Sandick, JHEP **1111**, 110 (2011), 1108.0448.

[14] R. D. Peccei and H. R. Quinn, Phys. Rev.D **16**, 1791 (1977).

[15] R. Peccei, Lect.Notes Phys. **741**, 3 (2008), hep-ph/0607268.

[16] L. F. Abbott and P. Sikivie, Phys. Lett. **B120**, 133 (1983).

[17] J. Preskill, M. B. Wise, and F. Wilczek, Phys. Lett. **B120**, 127 (1983).

[18] M. Dine and W. Fischler, Phys. Lett. **B120**, 137 (1983).

[19] S. Weinberg, Phys.Rev.Lett. **40**, 223 (1978).

[20] F. Wilczek, Phys.Rev.Lett. **40**, 279 (1978).

[21] J. E. Kim, Phys.Lett. **B136**, 378 (1984).

[22] K. Rajagopal, M. S. Turner, and F. Wilczek, Nucl.Phys. **B358**, 447 (1991).

[23] L. Covi, J. E. Kim, and L. Roszkowski, Phys. Rev. Lett. **82**, 4180 (1999), hep-ph/9905212.

[24] A. Brandenburg and F. D. Steffen (2004), hep-ph/0406021.

[25] A. Strumia, JHEP **1006**, 036 (2010), 1003.5847.

[26] K.-Y. Choi, L. Covi, J. E. Kim, and L. Roszkowski, JHEP **04**, 106 (2012), 1108.2282.

[27] H. Baer and A. D. Box, Eur.Phys.J. **C68**, 523 (2010), 0910.0333.

[28] H. Baer, A. Lessa, S. Rajagopalan, and W. Sreethawong, JCAP **1106**, 031 (2011), 1103.5413.

[29] K. J. Bae, H. Baer, and E. J. Chun, JCAP **1312**, 028 (2013), 1309.5365.

[30] H. Baer, A. Lessa, and W. Sreethawong, JCAP **1201**, 036 (2012), 1110.2491.

[31] H. Baer, A. D. Box, and H. Summy, JHEP **1010**, 023 (2010), 1005.2215.

[32] H. Baer, V. Barger, P. Huang, D. Mickelson, A. Mustafayev, et al., Phys.Rev. **D87**, 115028 (2013), 1212.2655.

[33] H. Baer, S. Kraml, and S. Kulkarni, JHEP **1212**, 066 (2012), 1208.3039.

[34] J. E. Kim, Phys.Rev.Lett. **43**, 103 (1979).

[35] M. A. Shifman, A. Vainshtein, and V. I. Zakharov, Nucl.Phys. **B166**, 493 (1980).

[36] S. Chang and K. Choi, Phys.Lett. **B316**, 51 (1993), hep-ph/9306216.

[37] A. Brandenburg, L. Covi, K. Hamaguchi, L. Roszkowski, and F. Steffen, Phys.Lett. **B617**, 99 (2005), hep-ph/0501287.

[38] G. Barenboim, E. J. Chun, S. Jung, and W. I. Park, Phys.Rev. **D90**, 035020 (2014), 1407.1218.

[39] C. S. Redino, Ph.D. thesis, SUNY, Buffalo (2015), 1506.08254, URL `http://inspirehep.net/record/1380201/files/arXiv:1506.08254.pdf`.

[40] J. E. Kim and G. Carosi, Rev.Mod.Phys. **82**, 557 (2010), 0807.3125.

[41] K. Olive et al. (Particle Data Group), Chin. Phys. **C38**, 090001 (2014).

[42] S. Chatrchyan et al. (CMS Collaboration), JHEP **1211**, 172 (2012), 1207.0627.

[43] G. Aad et al. (ATLAS Collaboration) (2014), 1409.5542.

[44] S. Ambrosanio, G. L. Kane, G. D. Kribs, S. P. Martin, and S. Mrenna, Phys.Rev. **D54**, 5395 (1996), hep-ph/9605398.

[45] L. Covi, in *2011 Electroweak Interactions and Unified theories*, edited by E. Auge, J. Dumarchez, and J. T. Thanh Van (2011), pp. 381–389.

[46] M. Dine, W. Fischler, and M. Srednicki, Phys.Lett. **B104**, 199 (1981).

[47] A. Zhitnitsky, Sov.J.Nucl.Phys. **31**, 260 (1980).

[48] M. Srednicki, Nucl.Phys. **B260**, 689 (1985).

[49] D. B. Kaplan, Nucl.Phys. **B260**, 215 (1985).

[50] M. Arik et al. (CAST), Phys. Rev. **D92**, 021101 (2015), 1503.00610.

[51] E. Armengaud et al., JINST **9**, T05002 (2014), 1401.3233.

[52] M. S. Turner, Phys.Rept. **197**, 67 (1990).

[53] G. G. Raffelt, Phys.Rept. **198**, 1 (1990).

[54] T. Moroi and H. Murayama, Phys.Lett. **B440**, 69 (1998), hep-ph/9804291.

[55] G. F. Giudice, E. W. Kolb, A. Riotto, D. V. Semikoz, and I. I. Tkachev, Phys.Rev. **D64**, 043512 (2001), hep-ph/0012317.

[56] D. Grin, T. L. Smith, and M. Kamionkowski, Phys.Rev. **D77**, 085020 (2008), 0711.1352.

[57] L. Covi, L. Roszkowski, and M. Small, JHEP **0207**, 023 (2002), hep-ph/0206119.

[58] P. Meade, M. Reece, and D. Shih, JHEP **1010**, 067 (2010), 1006.4575.

[59] P. W. Graham, D. E. Kaplan, S. Rajendran, and P. Saraswat, JHEP **1207**, 149 (2012), 1204.6038.

[60] G. Aad et al. (ATLAS), JINST **8**, P07015 (2013), 1305.2284.

[61] M. W. Cahill-Rowley, J. L. Hewett, A. Ismail, M. E. Peskin, and T. G. Rizzo (2013), 1305.2419.

[62] J. Alwall, R. Frederix, S. Frixione, V. Hirschi, F. Maltoni, et al., JHEP **1407**, 079 (2014), 1405.0301.

[63] H. Baer, S. Kraml, A. Lessa, and S. Sekmen, JCAP **1104**, 039 (2011), 1012.3769.

[64] J. Pumplin, D. R. Stump, J. Huston, H. L. Lai, P. M. Nadolsky, and W. K. Tung, JHEP **07**, 012 (2002), hep-ph/0201195.

[65] A. Alloul, N. D. Christensen, C. Degrande, C. Duhr, and B. Fuks, Comput.Phys.Commun. **185**, 2250 (2014), 1310.1921.

[66] C. Degrande, C. Duhr, B. Fuks, D. Grellscheid, O. Mattelaer, et al., Comput.Phys.Commun. **183**, 1201 (2012), 1108.2040.

[67] C. Duhr and B. Fuks, Comput.Phys.Commun. **182**, 2404 (2011), 1102.4191.

[68] R. M. Barnett, J. F. Gunion, and H. E. Haber, Phys.Rev. **D37**, 1892 (1988).

[69] N. D. Christensen, P. de Aquino, N. Deutschmann, C. Duhr, B. Fuks, et al., Eur.Phys.J. **C73**, 2580 (2013), 1308.1668.

[70] B. Fuks, Int.J.Mod.Phys. **A27**, 1230007 (2012), 1202.4769.

[71] B. Allanach, Comput.Phys.Commun. **143**, 305 (2002), hep-ph/0104145.

[72] A. Djouadi, J.-L. Kneur, and G. Moultaka, Comput.Phys.Commun. **176**, 426 (2007), hep-ph/0211331.

[73] M. Cacciari, G. P. Salam, and G. Soyez, Eur.Phys.J. **C72**, 1896 (2012), 1111.6097.

[74] T. Sjostrand, S. Mrenna, and P. Z. Skands, JHEP **0605**, 026 (2006), hep-ph/0603175.

[75] J. Thaler, *LHC Olympics, http://www.jthaler.net/olympicswiki/doku.php* (2006), URL `http://www.jthaler.net/olympicswiki/doku.php?id=lhc_olympics:analysis_tools/`.

[76] C. Redino, *http://github.com/csredino* (2015), URL `https://github.com/csredino`.

[77] I.-W. Kim and K. M. Zurek, Phys.Rev. **D89**, 035008 (2014), 1310.2617.

[78] E. H. Guillian (1999).

[79] R. Barbier, C. Berat, M. Besancon, M. Chemtob, A. Deandrea, et al., Phys.Rept. **420**, 1 (2005), hep-ph/0406039.

[80] T. Higaki, K. Nakayama, K. Saikawa, T. Takahashi, and M. Yamaguchi, Phys.Rev. **D90**, 045001 (2014), 1404.5796.

[81] T. J. LeCompte and S. P. Martin, Phys.Rev. **D84**, 015004 (2011), 1105.4304.

[82] H. K. Dreiner, M. Kramer, and J. Tattersall, Europhys.Lett. **99**, 61001 (2012), 1207.1613.

[83] M. Beltran, J. Garcia-Bellido, and J. Lesgourgues, Phys.Rev. **D75**, 103507 (2007), hep-ph/0606107.

[84] F. D. Steffen, Eur.Phys.J. **C59**, 557 (2009), 0811.3347.

[85] S. Hannestad, A. Mirizzi, and G. Raffelt, JCAP **0507**, 002 (2005), hep-ph/0504059.

[86] L. Roszkowski, S. Trojanowski, and K. Turzynski, JHEP **1411**, 146 (2014), 1406.0012.

[87] L. Roszkowski, S. Trojanowski, and K. Turzynski (2015), 1507.06164.

[88] A. Monteux and C. S. Shin, Phys. Rev. **D92**, 035002 (2015), 1505.03149.

[89] P. Ade et al. (Planck) (2015), 1502.01589.